

Review

Experimental Review on Friction Stir Welding of Aluminium Alloys with Nanoparticles

Cyril Vimalraj¹  and Paul Kah^{2,*} 

¹ Laboratory of Welding Technology, LUT University, FI 53851 Lappeenranta, Finland; Cyril.Vimalraj@student.lut.fi

² Division of Welding Technology, University West, 461 86 Trollhättan, Sweden

* Correspondence: paul.kah@hv.se

Abstract: To reduce environmental impacts and ensure competitiveness, the fabrication and construction sectors focus on minimizing energy and material usage, which leads to design requirements for complex structures by joining of similar and dissimilar materials. Meeting these industrial demands requires compatible materials with improved properties such as good weight-to-strength ratios, where aluminum (Al) and its alloys are competing candidates for various complex applications. However, joining Al with fusion welding processes leads to joint deterioration. Friction stir welding (FSW) produces joints at temperatures below the melting temperature, thus avoiding flaws associated with high heat input, yet requires improvement in the resultant joint properties. Recent studies have shown that nanoparticle reinforcement in FSW joints can improve weld properties. The main focus of this study is to critically review similar and dissimilar friction stir welding of AA5083 and AA6082 with carbide and oxide nanoparticle reinforcement. The study also discusses the effect of welding parameters on reinforcement particles and the effect of nanoparticle reinforcement on weld microstructure and properties, as well as development trends using nanoparticles in FSW. Analysis shows that friction stir welding parameters have a significant influence on the dispersion of the reinforcement nanoparticles, which contributes to determining the joint properties. Moreover, the distributed nanoparticles aid in grain refinement and improve joint properties. The type, amount and size of reinforcement nanoparticles together with the welding parameters significantly influence the joint properties and microstructures in similar and dissimilar Al welds. However, research is still required to determine the strengthening mechanism used by nanoparticles and to assess other nanoparticle additions in FSW of Al alloys.

Keywords: nanomaterials; microstructures; friction stir welding; aluminum alloys; AA5083; AA6082; reinforcing nanoparticles; dissimilar welding



Citation: Vimalraj, C.; Kah, P. Experimental Review on Friction Stir Welding of Aluminium Alloys with Nanoparticles. *Metals* **2021**, *11*, 390. <https://doi.org/10.3390/met11030390>

Academic Editor: Miguel Cervera

Received: 1 February 2021

Accepted: 19 February 2021

Published: 27 February 2021

Publisher's Note: MDPI stays neutral with regard to jurisdictional claims in published maps and institutional affiliations.



Copyright: © 2021 by the authors. Licensee MDPI, Basel, Switzerland. This article is an open access article distributed under the terms and conditions of the Creative Commons Attribution (CC BY) license (<https://creativecommons.org/licenses/by/4.0/>).

1. Introduction

Efficient production and reduced energy consumption have become a top priority of government policies aimed at promoting sustainable development. In efforts to achieve environmental and economic sustainability, industries aim to implement solutions that use minimum resources, improve production processes, and develop enhanced materials. The requirement for minimal resource utilization means that fabrication designs are tending towards joints with complicated structures and joints of similar and dissimilar metals [1].

Welding is a widely used and critical joining process in fabrication industries and consumes a lot of energy and materials [2]. Conventional fusion welding processes use phase regulator transistorized type power sources that have high energy consumptions and require large cooling units. There are limited arc manipulation features and improving such technology is expensive [3]. Moreover, conventional fusion welding can result in occlusion of gases, porosity, slag inclusions, solidification cracks and other distortions, causing expensive reworks and usage of more materials [4]. Advancements in welding

processes have, however, made it possible to produce sound joints using techniques such as solid-state welding, adaptive welding, robotic welding, cold metal transfer, spray arc, the use of flux cored welding wire, weld seam sensors and inverter-based power supplies. These and other improvements have resulted in a reduction in distortion and joint defects and consequently a reduction in material and energy usage [5]. However, the nature of conventional fusion welding processes restricts their usage in dissimilar welding and welding of heat sensitive Al alloys by the high heat input. As aluminum and its alloys have high thermal and electrical conductivities, the use of fusion welding processes has resulted in hot cracking and hydrogen embrittlement along the joint [5,6]. For instance, Da Silva and Scotti [7] showed that welding heat sensitive Al alloy AA5082 using pulsed gas metal arc welding process (GMAW) showed numerous porosity formations. Moreover, the usage of the double pulsed GMAW process tends to reduce the porosity formation compared to pulsed GMAW. However, the process cannot avoid porous formation. For the case of dissimilar welding, a study showed that welding of AA5083 to AA6061 using tungsten inert gas welding (TIG), metal inert gas welding (MIG) and FSW resulted in better properties in FSW joints compared to fusion welding processes. Moreover, the FSW joint had fine grain structures unlike joints made with fusion welding processes [8].

As no melting is involved in solid state welding, solid state techniques can overcome the shortcomings of fusion welding in production of similar and dissimilar weld joints [9]. The friction stir welding process is a more common and emerging process in solid state processes. In FSW, heat for welding is generated with pressure applied between the rotational tool and base metal, leading to plastic deformation without melting of the base metal and without change in the primary microstructure of the base metal. Moreover, welding by fusion welding processes results in eminent microstructural transformation and mechanical properties, which can be avoided in the FSW process. An experimental study of AA6061 with Al_2O_3 reinforcement using fusion and friction stir welding revealed that the high heat input of the fusion welding process led to dissociation of the Al_2O_3 composite, leading to brittle Al_4C_3 formation through the reaction between molten liquid and SiC. However, in the case of the friction stir welding process, there were no significant changes except that the Al_2O_3 particle size decreased and number of particles per unit area in the thermo-mechanically affected zone (TMAZ) region increased. This could be due to the agglomeration of Al_2O_3 particles and the inability of particles to orient with semisolid metal flow. In terms of mechanical properties, the hardness shown in the fusion zone was 70 HV, highlighting a softening effect in comparison to the hardness of the base metal (120 HV). On the other hand, the FSW joint showed that the hardness was similar to the base metal 100–140 HV in the stir zone; however, hardness increased in the TMAZ due to clustering of Al_2O_3 particles [10,11]. A schematic of FSW is shown in Figure 1. For increasing heat input, increasing the rotation speed or decreasing the travelling speed of the tool leads to better plastic material flow and the formation of a wider weld nugget (WN) [12,13].

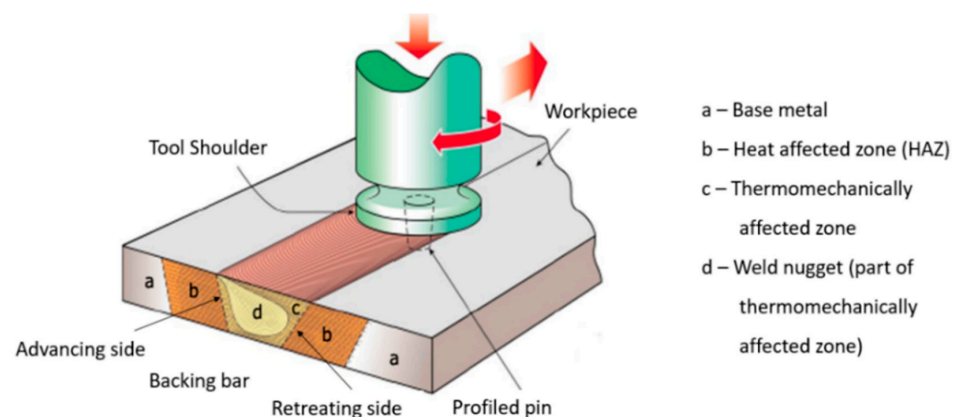


Figure 1. Schematic of the friction stir welding process.

Demanding applications such as those found in the marine, railway, automobile and aerospace industries demand a compatible material with desirable properties such as a good strength-to-weight ratio, high fatigue strength, and superior wear and corrosion resistance. Due to its inherent properties of good strength-to-weight and good corrosion resistance, aluminum and its alloys have been shown to be a viable and, in some cases, superior alternatives to steel. For instance, increasing concerns about resource usage have led to demands for improvement in fuel economy, triggering efforts to reduce the weight of vehicles. As a rule of thumb, in automotive industries, a 10% reduction in weight improves fuel economy by approximately 5.5%, and consequently usage of structural lightweight materials is highly desirable. Al has been one of the candidates used to provide good strength-to-weight ratios, so some of the engine parts have been fabricated by using Al alloys [14]. The 5x and 6x series of aluminum alloys have been employed for external structures and closure panels of vehicles and, as can be seen from Figure 2, have better density ratios than steel alternatives. Research is being carried out on 7x series Al alloys with the additions of scandium and zirconium for usage in engine cylinders to lower fuel consumption [15]. Corresponding with the automobile industry, the aerospace and the shipbuilding industries are also attempting to reduce pollutant emissions and structural costs through the use of Al alloy components in aircrafts and ship hulls [16]. For example, ferries produced using Al alloys have strengths equal to ferries made with steels for approximately half the weight, which increases fuel economy [17,18]. In recent years, various advanced Al alloys such as Al-Cu-Li, Al-Zn-Mn alloys, Al 7x series, Al 8x series and Al composites have been developed. These alloys exceed the requirements of current and foreseeable future demands [19]. For instance, the Al alloy Al-Cu-Li has been used in aeronautic applications, such as in aircraft wings, for its density ratio to mechanical resistance [20]. Although Al alloys have desirable characteristics, reduction in material usage of fabricated structures also requires welding of complex joints and joining of similar and dissimilar Al alloys.

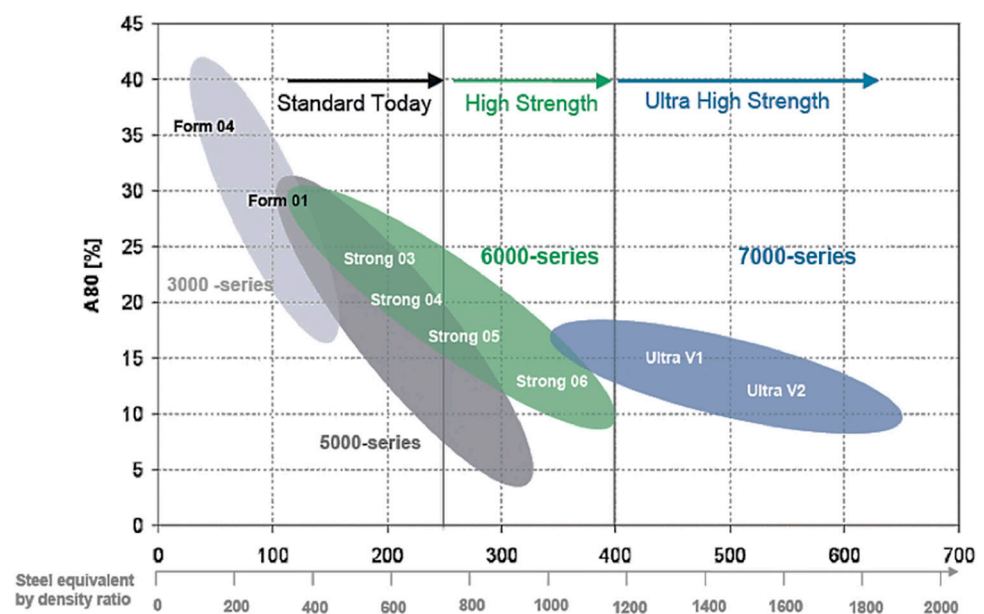


Figure 2. High strength aluminum sheets used for body structures in automotive industries [15].

Employment of fusion welding processes in welding of similar and dissimilar Al alloys results in poor weldability and can encounter problems such as weld solidification cracking, porosity, microstructural segregation from low melting eutectic formation, liquid cracking and brittle intermetallic formations. In addition, the mechanical properties of the joints can be reduced by coarse grain microstructural formations [21–23]. Studies suggest that welding of Al alloys using the GTAW process causes porosity formation and reduction

in tensile strength, due to a decrease in dislocation density and porosity formation leading to joint fractures [24]. However, the FSW process occurs below the melting temperature of the Al alloys, resulting in avoidance of metal solidification defects, less deformation, porosity and cracks, and improved mechanical integrity of the joints [25]. For example, a study showed that welding of Al-Cu-Li alloys using GTAW and FSW had joint formation with no defects. However, considering the mechanical joint strength, the FSW joint had better hardness properties (i.e., 120–130 HV from stir zone (SZ) to base metal) compared to GTAW joint (i.e., fusion zone –70 HV and base metal –130 HV). Moreover, the softening effect (i.e., reduction in hardness value) along the Heat-Affected Zone (HAZ) region in the GTAW joint has been compared to the FSW joint [20].

As aerospace industries focus on implementing lightweight structures in wing panels, FSW of 7x aluminum alloys is being evaluated for implementation. FSW 7x Al series showed that the tensile strength of the joint improved 5.33% of the parent metal [26]. Moreover, the marine industries require storage tanks and pipelines in ferries with lightweight materials such as Al alloys. The Al alloy AA6061, which joins with low heat input, was selected, where FSW was opted for as the fusion welding process uses filler material that increases the weights of the structures [27]. The study showed the FSW of AA6061 increased in ultimate tensile strength (160 MPa) with increased tool rotational speed, welding speed and tool axial force [28]. In recent decades, studies have been conducted on FSW of similar and dissimilar Al alloys with the aim of optimizing the welding parameters and improving weld properties. Welding of 7x series in Al alloys has been used for high stress components. The joints produced by FSW of Al alloys had minor reductions in strength compared to the base metal [26]. Moreover, another study also indicates that 7x series of Al alloys have reductions in mechanical strength due to the temperature variation in weld produced by the tool geometry and tool size. This temperature difference caused variation in grain size, precipitation size as well as distribution of particles, resulting in decrement in ductility, tensile strength as well as yield strength [10]. Research showed that the FSW welding parameters such as pin size, tool rotational speed and tool traverse speed has adverse effects on the formation of the microstructure and properties of the joint. With a low rotational speed and constant traverse speed, the small sized pin had better mechanical properties compared to the large sized pin [26]. Apart from the tool geometry and welding parameters, studies also suggest that using various reinforcement materials in the stir zone can prevent abnormal grain growth and lead to grain refinement, as well as enhancement of the mechanical properties of Al joints [29,30].

Nanoparticles have commonly been used as reinforcement particles, as their size leads to uniform dispersion, grain refinement and improved joint properties. For example, nanoparticles coated on base metals and coated on electrodes in fusion welding (i.e., gas metal arc welding and gas tungsten arc welding) produced joints with improved microstructural formations by grain refinement as well as and improved mechanical properties [31]. In addition to fusion welding processes, nanoparticles have also been incorporated in FSW of Al alloys [22,23]. The incorporation of nanoparticles in FSW joints improved the weld mechanical properties and microstructures by grain refinement [8]. To incorporate nanoparticles, ethanol was mixed with the reinforcing nanoparticles in a slurry and the specimens were machined with half grooves at the joining face plate. An example groove is shown in Figure 3. To prevent reinforcing nanoparticles being ejected out of the groove during welding, a pin-less tool was passed along the groove [32,33]. Another reason for incorporation of nanoparticles in the stir zone (SZ) is to aid stiffness and improve wear resistance in Al alloys [34].

As recent studies focus on application of nanoparticles in the FSW process and composite matrix formation and its effects on mechanical properties, they do not provide the correlation of nanoparticle selection with its effect in terms of the improvement of microstructure and properties. Moreover, only limited research has been conducted on dissimilar aluminum joints with nanoparticle reinforcement. This paper critically reviews the effects of incorporating carbide and oxide nanoparticles in friction stir welding of

the Al alloys AA5083 and AA6082 individually and assesses the effects on joint integrity. Moreover, the effects of carbide and oxide nanoparticles on microstructural formation and joint properties have also been highlighted as well as recent trends in welding of Al alloys using FSW with nanoparticle incorporation. The paper focuses on the influence of welding parameters such as traverse speed, rotational speed and number of passes. This article also discusses the dissimilar welding of AA5083 and AA6082 using FSW with and without nanoparticle reinforcement. The results of these nanoparticle reinforced similar and dissimilar AA5083 and AA6082 Al alloy series joints have been compared with joints without nanoparticle reinforcement.

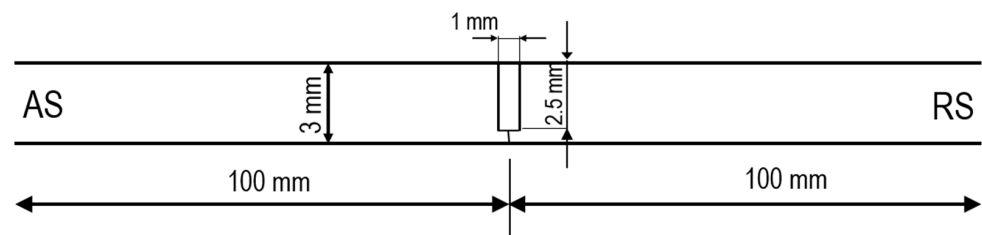


Figure 3. Example schematics of groove formation for usage in reinforcing nanoparticles.

2. Friction Stir Welding of Al Alloys Using Nanoparticles

The demand for welding of similar Al alloys has increased. For instance, in automobile industries, welded steel is being replaced by Al in key components that require flawless weld joints, such as pistons, cylinder heads and brake calipers [9,18]. When welding Al, fusion welding processes can produce joints with flaws, which can result in a reduction in mechanical properties due to high heat input. However, FSW can produce flawless Al joints with minimum heat input and minimum energy usage [12]. For instance, research showed that mechanical strength improved in 5x series Al joints using the FSW process through varying the traverse speed and rotational speed of the tool [35]. Nevertheless, the FSW process can cause a reduction in weld joint properties, which is undesirable and requires attention. Several studies have investigated the feasibility of improving FSW Al joint properties using reinforcement materials in the joint [32–34]. Al joints reinforced with nanoparticles showed reduction in grain size and improved tensile strength in the joint. For example, the FSW of AA5052 with SiC nanoparticles showed grain refinement with SiC acting as a nucleation site and providing a pinning effect on the grain boundaries, leading to increased hardness compared to joints without nanoparticle reinforcement [36].

However, reinforcement using nanoparticles has minor issues such as introducing nanoparticles in the FSW process, dispersion of nanoparticles in the weld and the selection of nanoparticles. For instance, to introduce the nanoparticles as reinforcement in the FSW process required groove preparation. Even though the open groove preparation assisted the incorporation of nanoparticles as a reinforcement, the pressing of the FSW tool resulted in a splatter of nanoparticles across the weld region, leading to nonhomogeneous distribution [23,37,38]. To reduce the spatter of nanoparticles from the groove, research has been conducted producing nanoparticle paste by mixing the nanoparticles with ethanol solution in order to avoid inconsistent distribution of nanoparticles [33,39]. Moreover, some studies showed that, before welding, a pinless tool passed along the groove with nanoparticle reinforcement to evade expulsion of nanoparticles [36,40]. More studies are required that use this method of introducing nanoparticles to the weld with homogeneous distribution. Another complication in using nanoparticles as a reinforcement is agglomeration in the weld region, which leads to reduction in joint strength [35,37]. This tendency of nanoparticles to cause agglomeration is due to the high surface area causing increase in space between particles, thereby resulting in pores [41]. Experiments are being carried out using the FSW process by changing tools geometries and sizes as well as increasing the number of passes along the joint for reducing the agglomeration. Studies showed that agglomeration of nanoparticles in the weld reduced from 256 to 219 nm through varying

the tool geometry and increasing as two passes along the groove [42,43]. Apart from the nanoparticle introduction to and dispersion in the weld, the nanoparticle selection also causes a problem in the FSW process. A study showed that friction stir welding of Al 6x series using Al_2O_3 nanoparticles causes joint formation with high microhardness compared to joints made using TiO_2 nanoparticles. Moreover, the joint using Al_2O_3 nanoparticles had a higher tensile strength compared to the TiO_2 nanoparticle joint, which is due to the high density of Al_2O_3 [44]. The amount of nanoparticle reinforcement has a vital effect on the weld joint formations. So, more studies are required to establish a method of using nanoparticles in the weld and reducing spatter of nanoparticles surrounding the groove.

The Al alloys AA5083 and AA6082 have been widely used in the marine and automobile industries due to their desirable properties and weldability [19]. The following sections give an overview of friction stir welding of AA5083 and AA6082 with nanoparticle reinforcement and its effect on joint properties.

2.1. Friction Stir Welding of 5x Series Al Alloy

The AA5083 alloy has good corrosion resistance, mechanical properties and fatigue-fracture resistance, and the alloy is used in applications such as panels in boats and trains, storage tanks, pressure vessels, piping and components in automobile and aerospace [45]. However, welding of AA5083 alloy with gas tungsten arc welding (GTAW) can result in coarse grain formation along the HAZ, leading to softening in the HAZ region. As a result of dissolution of strengthening precipitates and high heat input, joint failure occurs in the weld metal [46].

FSW has a low heat input and does not melt the base metal, and FSW of AA5083 has resulted in improvement of tensile strength and fine microstructural grain formations without any flaws [47]. The microstructural formation as well as weld joint properties are enhanced by heat input through the FSW tool rotation and traverse speed. For instance, Klobcar et al. [48] have shown that FSW of AA5083 with low heat input (i.e., high traverse speed and low rotational speed of the tool) results in an elongated cavity, as shown in Figure 4c. Use of optimal heat input by changing the welding parameters improved joint formation without introducing defects (Figure 4a). High heat input (i.e., low traverse speed and high rotational speed of tool) resulted in recrystallization and oxidation, causing grain growth and decrease in joint mechanical properties without any distortion, as shown in Figure 4b. However, some studies also showed that for the FSW of 5x series Al alloys, the mechanical properties were enhanced by a high traverse speed and lower rotational speed [49].

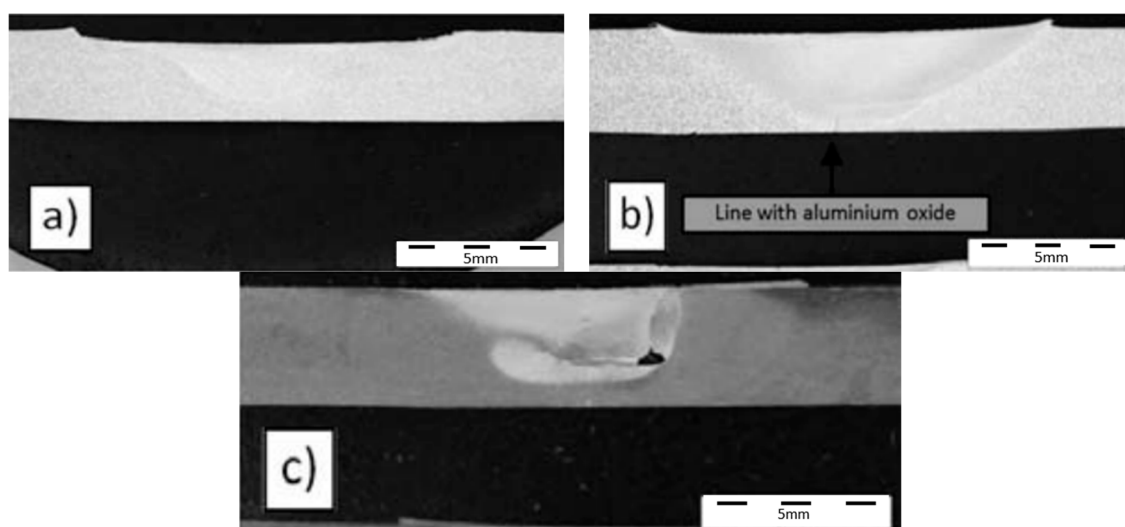


Figure 4. Macroscopic image of AA5083 joints by (a) optimal heat input, (b) high heat input and (c) low heat input [48].

Recent research has shown that the use of reinforcement particles in FSW can improve weld properties, aid microstructure formations and reduce joint defect formation [22,50]. For instance, Saeidi et al. [30] showed that the mechanical and corrosion resistances of dissimilar 5x series Al joints were improved by utilization of alumina nanoparticles. These improvements were due to dynamic recrystallization, causing the formation of a new nucleation site, thereby reducing grain growth and acting as a reinforcement against corrosive environments. Apart from nanoparticle reinforcement, optimization of welding parameters can also enhance joint properties by promoting uniform distribution of reinforcement particles while maintaining low heat input. For example, an AA5086 joint reinforced with SiC particle reinforcement in the joint, welded with a single pass, had inferior properties. However, increasing the number of passes led to an improvement in tensile properties and reduction in grain size compared to a joint without nanoparticle reinforcement, which can be seen in Figure 5 [51].

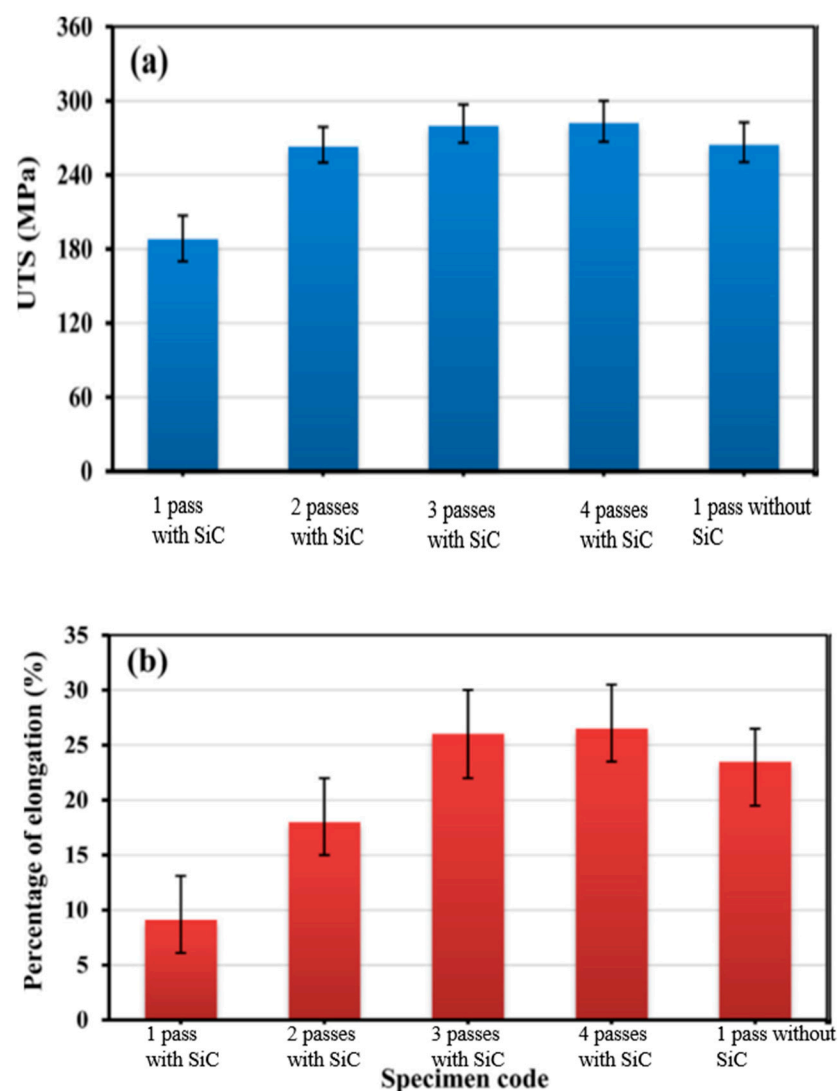


Figure 5. Mechanical properties of (a) tensile strength and (b) elongation in Friction stir welding (FSW) joints with SiC reinforcement [51].

Thereby, the effect of carbide and oxide nanoparticle reinforcement on welding AA5083 in terms of microstructure and joint properties are outlined in the following section, also considering the influence of welding parameters on reinforcement particles in the joint.

2.1.1. Effect of Welding Parameters on Joint Integrity of FSW Welds with Carbide and Oxide Nanoparticle Reinforcement

Increasing the number of passes in FSW of AA5086 with SiC nanoparticle reinforcement improved the mechanical joint properties and reduced grain size [51] and a similar effect has also been noted in FSW of AA5083 with TiO₂ nanoparticles [52]. Moreover, the AA5083 joint reinforced with TiO₂ nanoparticles welded in a single pass exhibited agglomeration of particles in the WN but increase in the number of passes tended to produce a more uniform distribution of the nanoparticles around the WN.

The traverse and rotation speeds of the tool play a vital role in the dispersion of nanoparticles in joints [22,50]. For instance, the use of two passes in FSW of AA5083 with TiC and SiC nanoparticle additions, with low rotational speed (i.e., 750 rpm) and high traverse speed (85 mm/min), showed high agglomeration of nanoparticles at the WN edge. Increasing the rotational speed (i.e., to 1500 rpm) and using a high traverse speed (85 mm/min) and three passes resulted in low agglomeration. However, increased rotational speed and decreased traverse speed (19 mm/min) produced homogeneous distribution of particles and no agglomeration was found, as can be seen in the macro image of the joint shown in Figure 6 [53].

Specimen with SiC reinforcement Specimen with TiC reinforcement



Weld joint using 750 RPM, 85mm/min & 2 passes



Weld joint using 750 RPM, 85mm/min & 2 passes



Weld joint using 1180 RPM, 85mm/min & 3 passes



Weld joint using 1180 RPM, 85mm/min & 3 passes



Weld joint using 1500 RPM, 85mm/min & 3 passes



Weld joint using 1500 RPM, 85mm/min & 3 passes



Weld joint using 1500 RPM, 19mm/min & 3 passes



Weld joint using 1500 RPM, 19mm/min & 3 passes

Specimen without reinforcement



Weld joint using 750 RPM, 75mm/min & 1 pass

Figure 6. Macroscopic image of AA5083 joints with and without nanoparticle reinforcement [53].

In addition to the friction stir welding parameters, the tool geometry also has a critical effect on dispersion of material flow and plastic deformation [54]. For example, Palani et al. [55] showed that the hexagonal tool shaped pin with SiC nanoparticles, com-

pared to a square or cylindrical tool, showed joint formation with no porosity, no tunnel defect and no crack formation as well as no agglomeration. However, the AA5083 joints with Al_2O_3 nanoparticles and without nanoparticle reinforcement showed tunnel defect and cracks. These defect formations could be due to the improper dilution of nanoparticles and improper dynamic recrystallization by high welding speed and the tool's pin length [56]. So, the shapes of tool geometry and the classification of nanoparticle reinforcement have variable effects on the joint properties during dynamic recrystallization.

2.1.2. Effect of Carbide and Oxide Nanoparticles on Microstructural Formation

When considering microstructural formation, nanoparticle reinforcement in Al joints tends to reduce the grain size [8]. With SiC and TiC nanoparticles, the equiaxed grain size in the joint was reduced compared with grain sizes in joints without nanoparticles. The grain size produced with TiC nanoparticles was smaller than the grain size when using SiC nanoparticles [53]. This reduction in grain size could be a result of dynamic recrystallization as well as a greater pinning effect on the grain boundaries with TiC nanoparticle reinforcement [22,23,29].

By using TiO_2 nanoparticles with a single pass, the grain size was slightly reduced compared to the grain size attained without nanoparticles. However, the grain size was further reduced by increasing the number of passes on the joints with TiO_2 nanoparticles [52]. This grain size reduction was also caused by the pinning effect on the grain boundaries [29]. A similar effect on grain size reduction with increasing the number of passes has also been noticed in AA5083 joints with ZrO_2 nanoparticle reinforcement [57].

In FSW of AA5083, the heat generated by friction and deformation causes recrystallization of microstructures in the WN due to low density of dislocation in the cell. However, in the TMAZ region in Al alloys there is insufficient strain for recrystallization, leading to dissolution of precipitated microstructures and causing high density dislocation along subgrain boundaries [47,58]. A similar effect appeared on the AA5083 joint reinforced with TiO_2 nanoparticles, due to higher density dislocation in the TMAZ [52]. This increase in density of cell dislocation could be due to the difference in the thermal coefficient of TiO_2 and AA5083 [59]. However, the joints with carbide (SiC and TiC) nanoparticle addition have only been slightly affected by dislocation of the cell in the WN and TMAZ, as the carbide nanoparticles are pinned along the grain boundaries [53].

Addition of carbide nanoparticles, such as SiC and TiC, causes particles to gather around and inside the intermetallic compounds [53], which is shown in Figure 7. These SiC nanoparticle agglomeration formations in intermetallic compounds could occur due to the reaction with the alloying element [36]. According to the literature [23,46,48], Mg_2Si , Mg_2Al_3 , $\text{Cr}_2\text{Mg}_3\text{Al}_{18}$, Al_2Cu , Al_2CuMg , TiAl and $\alpha\text{-Ti}_3\text{Al}$ were the intermetallic compounds observed in the base metal AA5083. Joints with carbide (i.e., TiC and SiC) and oxide (ZrO_2) nanoparticle additions had similar intermetallic compound formations as the joints without reinforcement [53,57]. However, Mg_2Al_3 intermetallic compounds were not found in the joints of carbide nanoparticles [53]. This could be due to the dilution by the heat generated by friction, leading to a reduction in strength of the joint.

Hence, it can be derived from the studies that the carbide nanoparticles underwent reductions in grain size compared to oxide nanoparticles. However, the oxide nanoparticles had their grain sizes reduced with an increased number of passes on the AA5083 joint. The increase in dislocation density at the WN was not affected by carbide nanoparticles; however, oxide nanoparticles tend to increase the dislocation density by the TiO_2 nanoparticles thermal coefficient. Similar intermetallic compounds were found in the joints with and without nanoparticle reinforcement; although, some intermetallic particles were diluted by frictional heat.

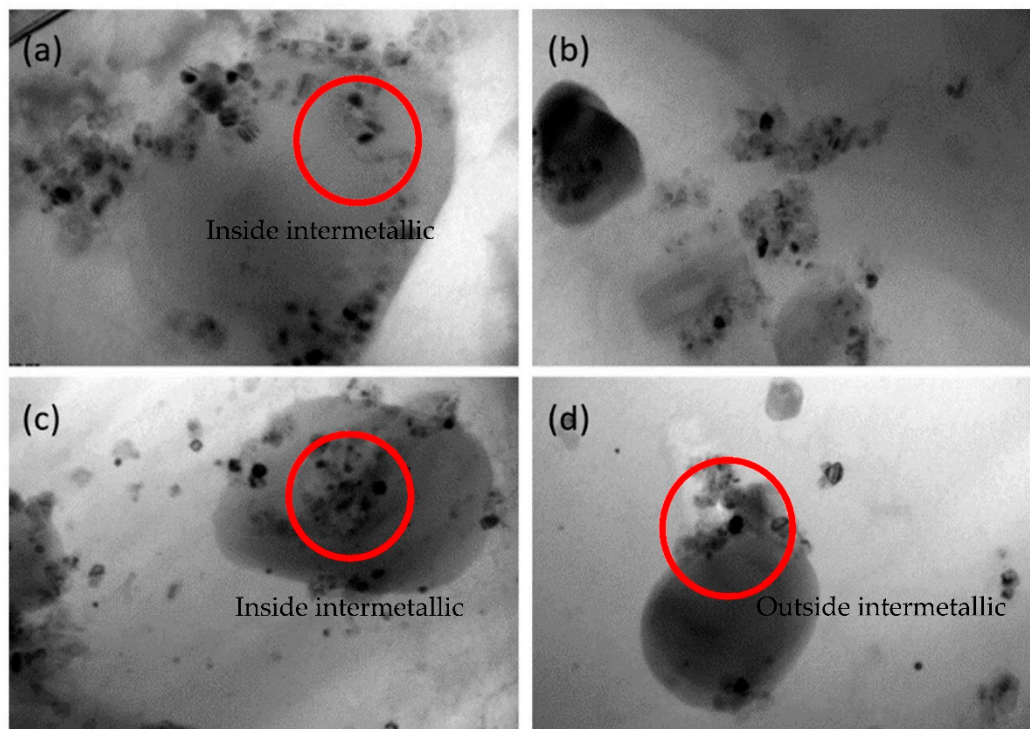


Figure 7. Reinforcement of nanoparticles: (a,b) SiC inside intermetallics; (c) TiC inside intermetallics; (d) TiC around intermetallics [53].

2.1.3. Effect of Carbide and Oxide Nanoparticles on Mechanical Properties

As per the Hall–Petch relation [23], with a reduction in the grain size, the hardness property tends to increase. In the AA5083 joint with SiC, TiC, ZrO₂ and TiO₂ nanoparticle additions, the joint with TiC had the smallest grain size followed by the joint with SiC nanoparticles [53], and the joints with ZrO₂ and TiO₂ nanoparticle reinforcements had slightly larger grain sizes [52,57]. In hardness, the joint reinforced with TiC nanoparticles had the highest hardness followed by the joint with oxide (i.e., TiO₂ and ZrO₂) nanoparticles; the lowest hardness value was found in the joint reinforced with SiC nanoparticles. These hardness increases by oxide nanoparticles compared to SiC nanoparticles could be due to the increase in passes, dislocation of the cell by thermal difference as well as hardness property of the oxide particle [30,31].

In addition to hardness, wear resistance is also a vital property, as AA5083 is used in applications in abrasive environments such as automobile components. Joints without nanoparticle additions have high weight losses as well as high wear rates [22,46]. TiO₂ nanoparticle reinforcement can improve the wear resistance, as shown in Figure 8 [52]. Increasing the number of passes tends to distribute the nanoparticles more uniformly, causing barriers to initiate cell dislocation for plastic deformation reduction [60].

When considering tensile and ductility properties, welds with carbide additions had high tensile strengths when compared to joints with oxide additions. A similar effect of improvement of tensile strength has been found in the joints with SiC and TiC nanoparticle additions, compared to joints with TiO₂ nanoparticle additions [52,53,57]. Moreover, the TiO₂ nanoparticle reinforced joint showed a reduction in tensile properties and elongation with an increase in the number of passes [52]. This reduction could be due to dislocation formations and hardening by strain differences [33]. In the case of carbide nanoparticle reinforcement in AA5083 joints, SiC nanoparticle reinforced joints had improved tensile strengths compared to joints without reinforcement and joints with TiC nanoparticles, which can be seen from Figure 9 [53]. This reduction in elongation and yield strength

could be due to the dissolution of strengthening precipitates as well as reinforcement of Ti nanoparticles, which have hard natures [61].

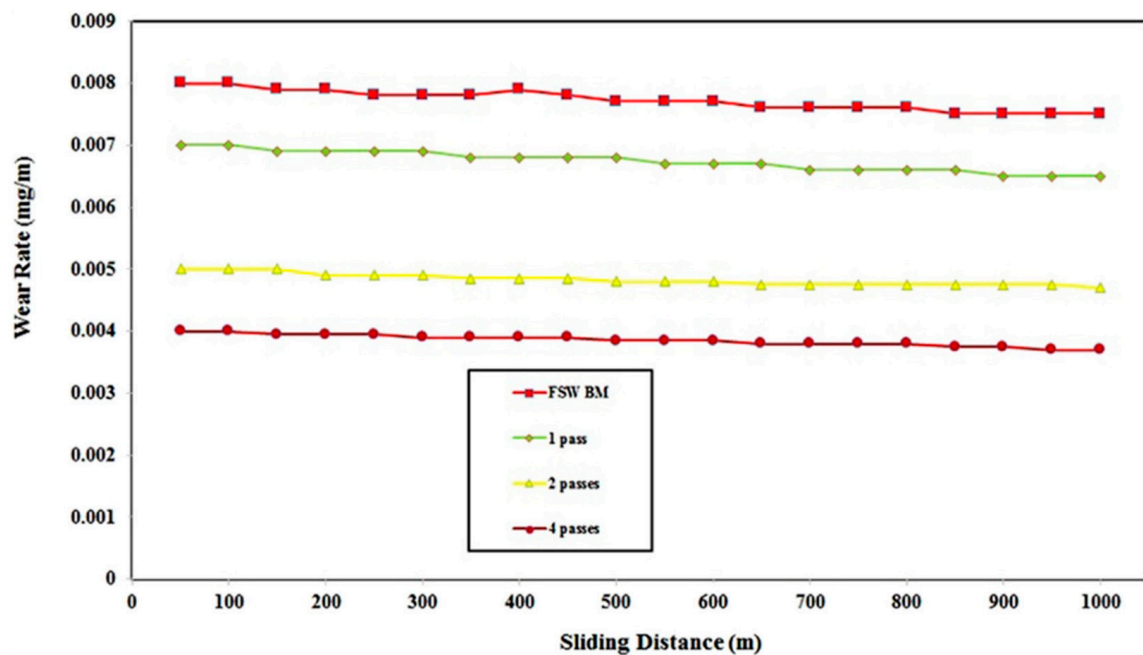


Figure 8. Wear rate of joints without and with TiO₂ nanoparticle reinforcement vs. sliding distance [52].

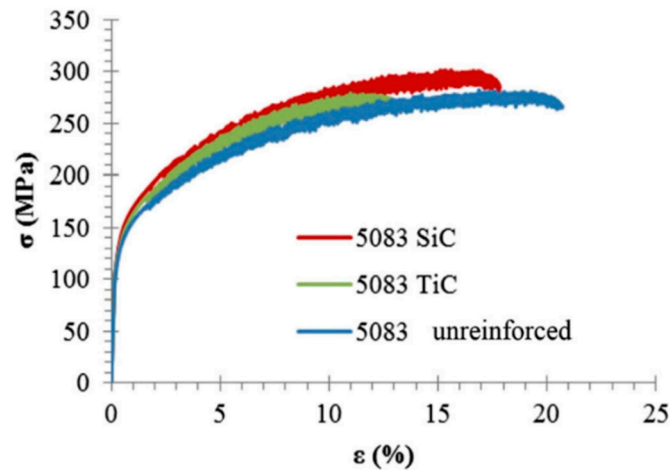


Figure 9. Stress–strain curve for joints without reinforcement and with SiC and TiC nanoparticle reinforcements.

2.2. Friction Stir Welding of 6x Series Al Alloy

Heat-treatable aluminum alloys (i.e., 6x series) are difficult to weld with fusion welding processes because the high heat input causes defects such as cracking, porosity and brittle solidification in the weld. These primary flaws are addressed in the FSW process by welding below the melting temperature of the alloy, resulting in low shrinkage and low residual stress in the joint, with improved mechanical properties [62]. In 6x series Al alloys, AA6082 is considered suitable for various industrial applications because of its good corrosion resistance and mechanical properties. However, welding with the gas metal arc welding (GMAW) process can result in porosity, fractures in the HAZ and reduction in mechanical properties such as tensile strength, hardness and impact strength [63]. Welding by the FSW process had no defect formations, resulting in improved tensile strength and

elongation [8,9,64]. In addition, hardness along the HAZ was improved with low heat when compared to the fusion welding process. Smaller grain sizes in the joint were observed with uniform distribution of precipitates; however, fractures occurred at the HAZ region of the friction stir welded AA6082 joint [65].

Studies showed that the friction stir welding parameters such as traverse speed, tool rotation speed and the geometry of the tool had adverse effects on the microstructure and mechanical properties when welding 6x series [1,8,54]. A study on AA6083 showed that with a high rotational speed and increased traverse speed of 115 mm/min, the yield strength improved due to the composition of small grain size. However, further increase in traverse speed resulted in tensile strength reduction and enlargement of grain size, due to high heat input for recrystallization [66]. Moreover, the shoulder and tool geometries as well as the number of passes have effects on the joint integrity. For instance, P. Cavaliere et al. [67] showed that increasing the number of passes on AA6082 causes the grain size to increase and the ultimate tensile strength to reduce, as well as soften (i.e., reduction in the hardness properties) the base metal. However, research showed that the hexagonal tool profile in FSW improves the tensile strength and hardness by uniformly distributing smaller grain sizes, compared to the joints formed with square and triangle tool profiles [64]. In addition to the improvements in properties achieved by changing the welding parameters, the softening effect occurred along the HAZ region of AA6082, causing fracture failure.

Studies have shown that the incorporation of refractory nanoparticles such as SiC and TiC in FSW processes for welding Al alloys have improved the mechanical properties as well as aided in microstructural formation by refining grains [33,68]. However, multi-walled carbon nanotubes (MWCNTs) have resulted in deterioration of properties as well as formation of brittle weld nuggets [23,68]. The following section overviews the effect of carbide nanoparticles incorporated in welding AA6082 for forming microstructures as well as influencing the properties of the joint.

2.2.1. Effect of Welding Parameters on Joint Integrity of FSW Welds with Carbide Nanoparticle Reinforcement

The softening effect on the AA6082 HAZ regions has been greatly influenced by welding parameters thereby determining the joint properties [66,67]. Studies have also shown that the carbide and oxide nanoparticle addition improved the mechanical properties (tensile and ductility) by the pinning effect on grain boundaries with the aid of welding parameters [29,31]. In the case of AA6082, S. K. Sing et al. [69] showed, with the addition of TiC nanoparticles in the weld groove at a higher rotational speed and higher traverse speed (i.e., 1200 rpm and 90 mm/min), that the tensile strength and hardness improved and the softening effect along the HAZ region reduced when compared to the joint without nanoparticle addition, which is shown in Figure 10. This occurred due to the uniform distribution of the TiC nanoparticles by high heat input with high rotational and traverse speeds of the tool. However, the TiC nanoparticles incorporated into joints at a low speed resulted in softening in the SZ as well as thermo-mechanically affected zone (TMAZ) [33,62].

P.N. Karakizis et al.'s [40] results also agreed with the welding parameters and the influence on nanoparticle distribution and improvement in joint properties. The study details the joint reinforced with both SiC and TiC nanoparticles and the influence of FSW welding parameters on the joint integrity is shown in Table 1.

From Table 1, it can be seen that low rotational speed, traverse speed and number of passes resulted in defect formations by nonhomogeneous distribution of nanoparticles. However, SiC and TiC used different traverse speed parameters for forming good joints [40,69]. This is due to the fact that SiC and TiC nanoparticles have different physical properties for dilution and dispersion [70].

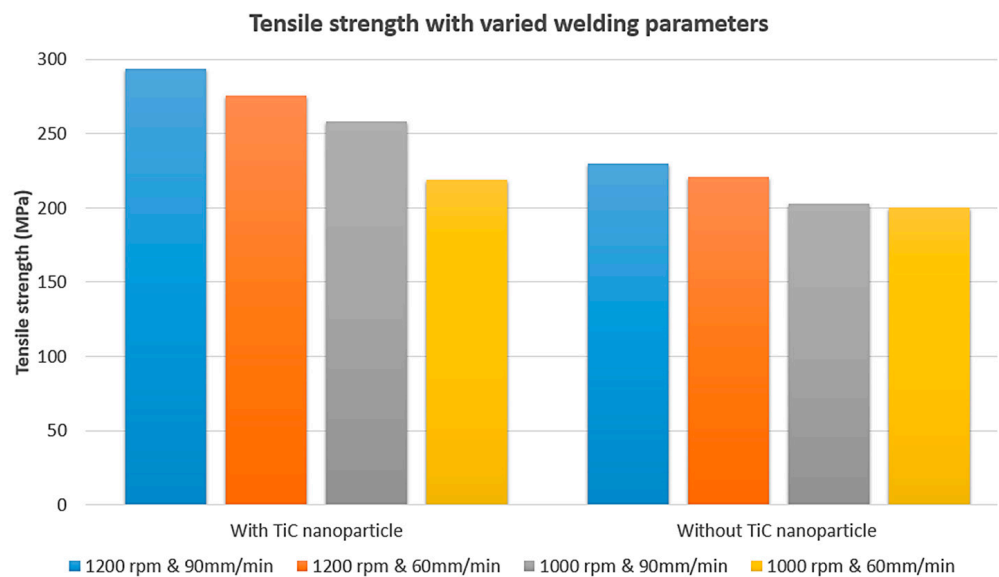


Figure 10. Joint tensile properties with TiC addition and variation in welding parameters.

Table 1. FSW parameters variation influence on nanoparticles distribution and its AA6082 joint characteristic.

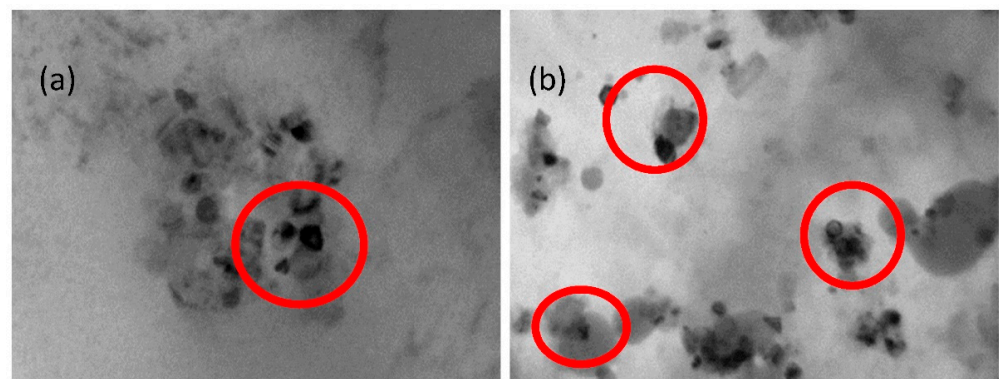
	Specimen	Effect
SiC nanoparticle	750 rpm, 85 mm/min and 2 passes	Porosity and agglomeration of nanoparticles
	1180 rpm, 85 mm/min and 3 passes (+++)	Porosity with agglomeration of particles.
	1500 rpm, 85 mm/min and 3 passes (+--+)	No porosity with agglomeration of particles.
	1500 rpm, 19 mm/min and 3 passes (+--+)	Uniform nanoparticle distribution and nil defect with better properties
TiC nanoparticle	750 rpm, 85 mm/min and 2 passes	Porosity and agglomeration of nanoparticles
	1180 rpm, 85 mm/min and 3 passes (+++)	Inhomogeneous distribution of nanoparticles with rich and poor region of particles
	1500 rpm, 85 mm/min and 3 passes (+--+)	Uniform nanoparticle distribution and nil defect with better properties
	1500 rpm, 19 mm/min and 3 passes (+--+)	No onion ring structure with inhomogeneous distribution forming poor and rich regions.

2.2.2. Effect of Carbide Nanoparticles on Microstructural Formation

The addition of nanoparticles in the friction stir welding process reduces the grain size through a pinning effect on the grain boundaries [8,34]. Similar effects have been found in the AA6082 joints by addition of TiC and SiC nanoparticles, where the tool's stirring action and plastic strain caused recrystallization, leading to pinning of nanoparticles on grain boundaries, thereby restricting the growth of grain [40,69]. From Table 2, the grain sizes in the weld nugget with the TiC nanoparticles underwent further grain size reduction when compared to the SiC nanoparticles. This could be due to the size of the nanoparticles—TiC (150–200 nm) and SiC nanoparticles (20–30 nm)—in addition to the stirring action, during which the nanoparticles were broken into further smaller sizes. TiC nanoparticles are more evenly distributed compared to SiC, which can be seen in Figure 11. Moreover, no agglomeration of SiC and TiC nanoparticles was found in the joints.

Table 2. Grain size in the weld nugget.

Specimen	Grain Size (μm)
Base metal	40
WN of reinforcement	5.5
WN with reinforcement of TiC nanoparticles	4.2
WN with reinforcement of SiC nanoparticles	5.1

**Figure 11.** No agglomeration (200 nm) of (a) SiC and (b) TiC nanoparticles in the weld nugget (WN) [40].

The literature on FSW of AA6082 [62,66,67] shows that softening along the HAZ by the high heat input results in the dissolution of strengthening intermetallic particles such as $\beta\text{-Al}_9\text{Fe}_2\text{Si}_2$ or $\beta\text{-Al}_5\text{FeSi}$ or $\alpha\text{-Al}_{12}\text{Fe}_3\text{Si}$. These stable intermetallic compound formations are replaced by changing the iron for magnesium or chromium, such as $\alpha\text{-Al}_{12}(\text{FeMn})_3\text{Si}$ or $\alpha\text{-Al}_{12}(\text{FeCr})_3\text{Si}$ or Mg_2Si . In the friction stirred AA6082 joints, dilution of β -phase intermetallics caused by the temperature rise during welding and low dislocation density by the dynamic recrystallization process resulted in the reduction in the joint mechanical strength. AA6082 joints with SiC and TiC nanoparticles had the same intermetallic compound formations as the joint without reinforcement. Three intermetallic particles, Mg_2Si , $\text{Al}_9\text{Mn}_3\text{Si}$ and $\alpha\text{-Al}_{12}(\text{FeMn})_3\text{Si}$, were identified in the WN by high contents of Mg, Fe and Si [40,69].

Studies have shown that the heat generation by friction and particle reinforcement is associated with the grain size, subgrain formation and dislocation density, which are responsible for determining mechanical properties [12,23,71]. However, research showed that the nanoparticle reinforcement had no effect on subgrain formation and only a small effect on dislocation density [40,69,71]. If there is high dislocation density, it could lead to subgrain formation by the high tool rotation and traverse speeds as well as during dynamic recrystallization [22,29,62].

In addition to the type of reinforcing nanoparticle, the volume of nanoparticle addition also aids in grain size formation [31,71]. For instance, FSW of AA6061 (i.e., alloy similar to AA6082 alloy) with SiC nanoparticles showed that increased volume fraction of nanoparticle reinforcement (from 14% to 29%) led to homogeneous dispersion, causing reduction in grain size as well as improvement in the mechanical properties [72].

2.2.3. Effect of Carbide Nanoparticles on Mechanical Properties

For mechanical properties, studies have shown that reinforcement particles have improved joint properties as well as surface properties [23,34]. The addition of SiC and TiC nanoparticles in the AA6082 joints improved the toughness and hardness properties. However, the type of carbide nanoparticle has an effect on the properties. For instance, the joint reinforced with SiC nanoparticles had improved toughness and elongation compared to the joints with TiC nanoparticles. However, the tensile strength of the joint reinforced with SiC nanoparticles drastically reduced compared to the joints without reinforcement

with TiC nanoparticles, which is shown in Table 3 [40]. This reduction in tensile and hardness properties could be due to the association of SiC nanoparticles with intermetallic compounds and the annealing region under high rotational speed and slow traverse speed [70,73].

Table 3. Tensile and toughness properties of the joint without and with SiC and TiC nanoparticle reinforcement.

Joint Specimen	Young's Modulus (GPa)	Yield Strength (MPa)	UTS (MPa)	Elongation (%)	Toughness (J/m ³)
Without nanoparticles	68.13 ± 2.71	146 ± 4.04	199.17 ± 5.8	3.79 ± 0.17	706.12 ± 13.28
With SiC nanoparticle	74.63 ± 4.94	106 ± 2.65	167.5 ± 7.49	5.97 ± 0.58	913.15 ± 22.35
With TiC nanoparticle	67.62 ± 3.6	139 ± 5.69	190.5 ± 4.82	3.95 ± 0.37	703.43 ± 9.39

The FSW joints with and without reinforcement nanoparticles fractured at the HAZ region, which could be due to low hardness and softening effect [67,69,72]. However, the joint reinforced with TiC nanoparticles showed better hardness when compared to the joints without reinforcement and joints with SiC nanoparticle reinforcement [40,69]. Moreover, the joints without reinforcement and with SiC nanoparticles tend to soften more along the HAZ region when compared to the TiC nanoparticle joint, which could be due to the dissolution of the strengthening precipitate and increased content of Mg and Si by SiC nanoparticles [74].

Studies also showed the amount of incorporating the nanoparticles have a greater influence on the mechanical properties of the joint. For instance, a study showed that, increased volume fraction of SiC nanoparticles in AA6061 alloy improved the hardness profile and tensile strength, which is shown in Figure 12 [72]. This improvement was mainly due to the absence of interface gap between the base metal and weld nugget.

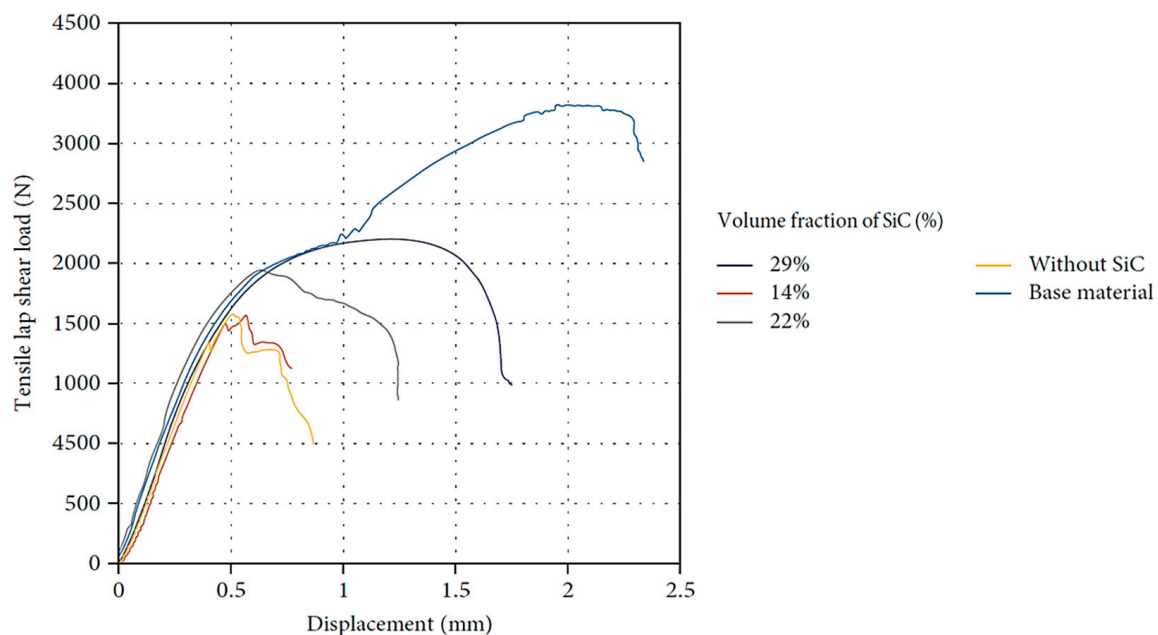


Figure 12. Tensile shear load with varying amounts of SiC nanoparticles [72].

Therefore, the studies show that the amount and type of nanoparticles as well as the optimum welding parameters play critical roles in achieving better joint properties in FSW of 6x series. Moreover, the SiC nanoparticles associate with intermetallic compounds to improve the tensile properties of joints. In the case of TiC nanoparticle reinforcement, the

hard nature of TiC increased the hardness property of the joint with aid of the welding parameter with a uniform distribution.

3. Friction Stir Welding of Dissimilar 5x Series and 6x Series Al Alloys Using Nanoparticles

FSW offers numerous advantages over the conventional fusion welding processes for welding dissimilar Al alloys. For instance, with easy automation, FSW produces joints with low distortions and good mechanical properties without the use of filler material or shielding gases. Moreover, the welding takes place below the melting temperature of the base metals, resulting in avoidance of the common problems associated with dissimilar Al alloys [75,76]. In 5x and 6x series Al alloys, AA5083 and AA6082 have been widely used in the marine industry for primary stiffener panels to reinforce the hulls of ships. Moreover, much research has been carried out on dissimilar Al welds 5x and 6x series to determine the relationship between the welding parameters and enhance the joint properties. As AA6082 is a heat-treatable Al alloy, the heat input results in deterioration of mechanical properties of the dissimilar weld joint [33].

Studies showed the heat input in FSW without nanoparticle reinforcement for dissimilar welding of AA5083 and AA6082 has been greatly influenced by the traverse speed and by the rotation speed of the tool. Moreover, the change in the tool rotation speed has a significant effect on the material flow in the stir zone. In addition to the rotational speed and traverse speed, the tool's advancing side and retreating side also have significant effects on the distortion and joint properties [77]. For example, M.J. Peel et al. showed that the dissimilar welding of AA5083 to AA6082 with AA5083 on the advancing side produced good mixing in the stir zone with no defect. However, having AA6082 as the advancing side resulted in a low level of mixing as well as defect formation such as voids or tunnels, which is shown in Figure 13 [76]. In addition, the joint with the tool advancing side in AA6082 showed a reduction in mechanical strength compared to the strength of the base metal. This could be due to decrease in the dislocation density in the weldment as well as the TMAZ [50].

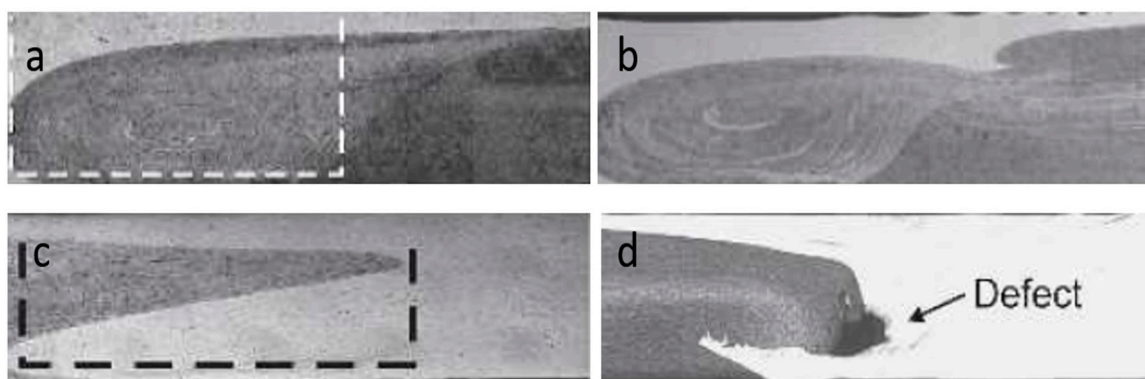


Figure 13. Macroscopic image of dissimilar joints with darker areas as AA5083: (a,b) AA5083 on advancing side; (c,d) AA6082 on advancing side with defect [76].

In the case of the mechanical properties of AA5083 to AA6082 joint, the joint produced with AA5083 as the advancing side resulted in a higher tensile strength compared to the joint produced with AA6082 as the advancing side, which could be due to the void defect formations. Moreover, for both dissimilar joints, the deformation occurred at the heat-affected zone of AA6082, causing joint failure. This could be due to the AA6082 alloy, as it relies on strengthening precipitates such as β'' - Mg_5Si_6 ; these precipitates (i.e., β'' - Mg_5Si_6) are unstable above 200 °C, causing rapid decrease in flow stress. In the AA5083 alloy, strengthening by the solid solution of Mg led to a gradual decrease in flow stress. Thus, the HAZ region in AA6082 tends to have a wide softening zone, resulting in

failure [76,78]. The increase in traverse and rotation speeds improved the ultimate tensile strength and elongation in failure of the dissimilar Al joint, which is shown in Figure 14. Recent research showed that the incorporation of nanoparticles in the dissimilar Al joints maintained the mechanical properties by retaining the strengthening precipitates and the suitable nanoparticles enhanced the mechanical properties of the joint [79,80].

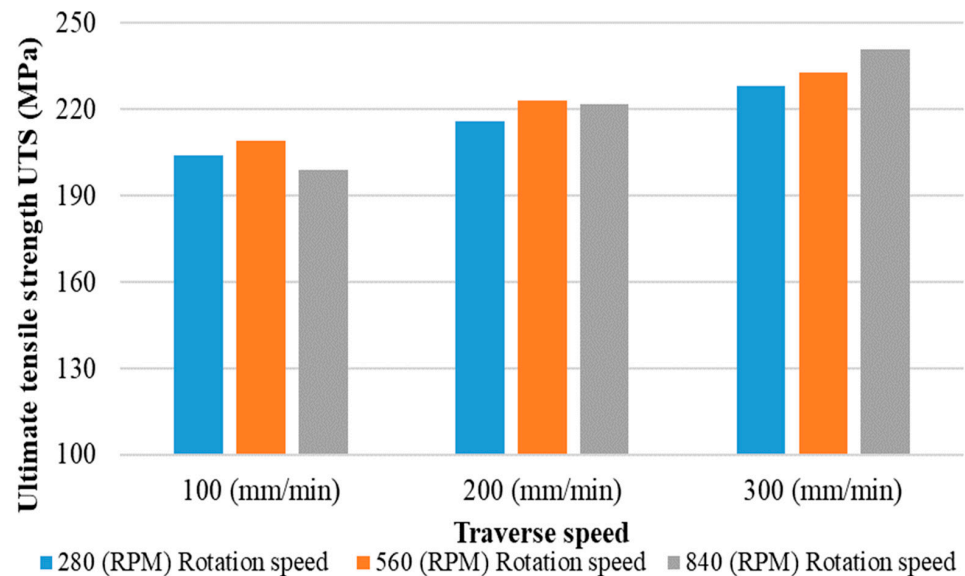


Figure 14. Ultimate tensile strength for the dissimilar Al joint with traverse and rotation speeds of the tool in FSW [76].

In addition to the tensile property, the hardness properties have also been improved by increasing the traverse speed compared to the joint formed with low traverse speed/low rotation speeds. However, by reaching the minimum hardness in the HAZ region, the softening effect remains the same irrespective of welding speed. This could be due to the changes in peak temperature and length of thermal cycle by the FSW tool encouraging dissolution or retaining of the solute [33,81].

In addition to the mechanical properties, corrosion resistance and residual stress play vital roles in joints, where the corrosion susceptibility and stress of dissimilar joints are high in the heat-affected zone [50]. The dissimilar Al joint has been more susceptible to corrosion in the heat-affected zone and TMAZ, which is due to Mg_2Si mismatch boundary [82]. As the dissimilar Al joint tends to soften in the HAZ region of AA6082, causing failure in the joint, studies show that incorporation of reinforcement particles in the stir zone could improve the joint integrity by improving mechanical properties as well as microstructural formation. Moreover, research also shows that incorporation of the nanoparticles for their uniform dispersion and grain boundary precipitation properties improved the microstructural formation, leading to better corrosion resistance and mechanical properties in the joint [33]. As there are various reinforcing nanoparticles, this section reviews the welding parameters with the effects of carbide nanoparticles such as TiC, SiC and others in dissimilar welding of AA5083 and AA6082.

3.1. Effect of Welding Parameters on Joint Integrity of FSW Welds with Carbide Nanoparticle Reinforcement

In FSW process, the traverse speed, rotation speed and advancing/retracting side of the tool in the base metal have great influences on dissimilar Al joint. Moreover, the number of passes in the joint also influences the microstructural formation and mechanical properties. As the dissimilar joints of AA5083 and AA6082 alloys showed defect formations with AA6082 as the advancing side, the joints which incorporated nanoparticles has a single pass with AA5083 as the advancing side and showed defects and agglomeration

of particles. Studies also showed that the reinforcement of nanoparticles with increase in number of passes led to more uniform distributions compared to a single pass along the joint [61]. For instance, D.I. Pantelis et al. [32] showed that the dissimilar welding of AA5083 to AA6082 using SiC nanoparticles with the optimal rotation speed and traverse speed (i.e., 750 RPM and 85 mm/min) had SiC nanoparticle agglomeration at lower areas and microvoids in the weld nugget with single pass. With the two passes along the same direction, the SiC nanoparticles slightly dispersed in the center and upper regions near the HAZ with small agglomeration. Moreover, along the same direction with a third pass still resulted in a very small agglomeration of nanoparticles in the upper region of the retreating side. However, with two passes changing the direction on the second pass (i.e., first pass with AA5083 as the advancing side and on second pass AA6082 with as the advancing side) resulted in a more uniform distribution in the weld nugget, characterized as an onion ring structure and no defect formation, which can be seen in Figure 15d.

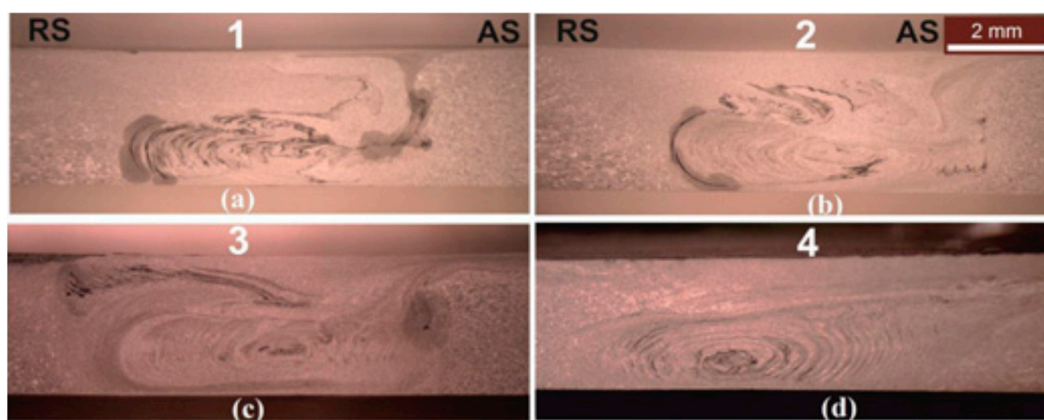


Figure 15. Macroscopic image of weld nuggets (a) with 1 pass, (b) with 2 passes along the same direction, (c) with 3 passes along the same direction and (d) with 2 passes in opposite directions [32].

A similar result was found for the dissimilar Al joint reinforced with TiC nanoparticles with optimal rotational speed of the tool, traverse speed (i.e., 750 RPM, 85 mm/min) and two passes along the same direction, leading to agglomeration of nanoparticles. However, increased rotation speed (i.e., 1180 RPM) of the tool along the same direction with three passes resulted in uniform distribution of TiC nanoparticles and lack of defect in the joint. Moreover, the dissimilar joint using TiC nanoparticles with the optimal rotation speed and with two and three passes in opposite directions showed severe agglomeration in the end of the stir zone and top of the HAZ region [33]. This agglomeration could be due to the tool shoulder and tool geometry causing the material flow in a downward movement [83]. However, by increasing the rotational speed to 1500 RPM with three passes in opposite directions resulted in the joint with uniform distribution of nanoparticles, no agglomeration and flawless joint formations [33].

3.2. Effect of Carbide Nanoparticles on Microstructural Formation

For microstructural formation, the dissimilar Al joint formed without the nanoparticle addition had average grain size of 13 μm in the weld nugget (WN) region. The grain size was small compared to the grain sizes of both the base metals AA5083 (26 μm) and AA6082 (40 μm), which was due to the dynamic recrystallization during friction stirring [71,81]. Studies showed that with incorporation of SiC nanoparticles into the joint causes an onion ring formation with concentric circles along the WN region, due to the vortex flow of material during welding. At the center of the weld nugget, the Si composition was high compared to the composition of Si in base metals. Moreover, the concentric region in the advancing side of the stir zone had a nanoparticle rich region and nanoparticle poor region as shown in Figure 16, where the rich region had a grain size of 7 μm and the poor region

had a grain size of 12 μm . Through further magnification, the areas of I and II were shown to have low Si contents and area III had enriched Si content [32]. So, the reduction in grain size in the rich region was due to the pinning effect of SiC preventing the grain growth [23].

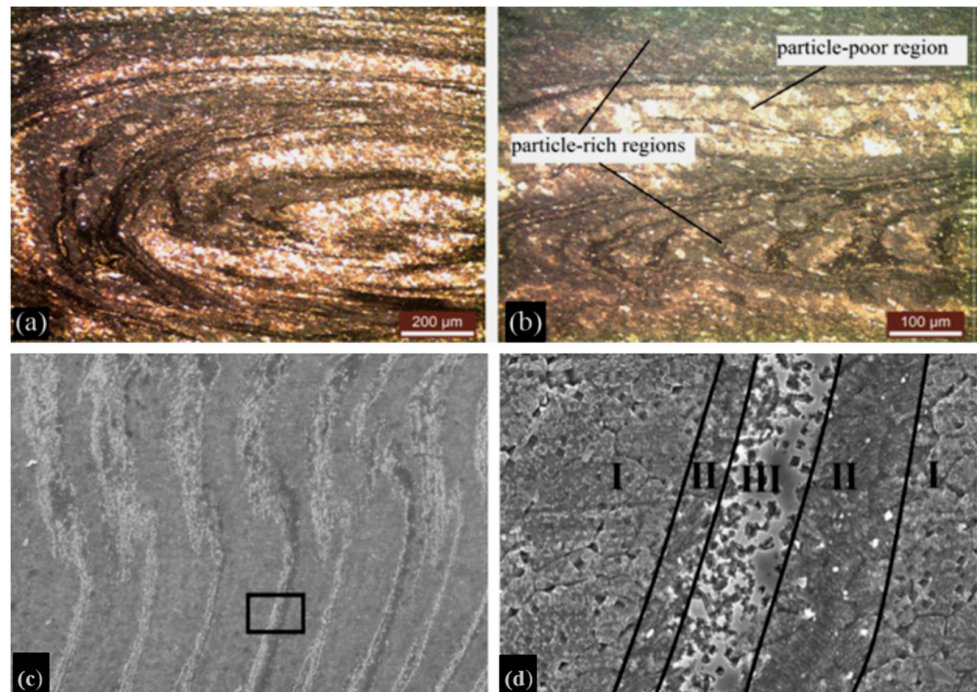


Figure 16. Microscopic image of the (a) center and (b) advancing side in weld nugget (c) concentric region and (d) area division in concentric region showing SiC rich and poor regions [32].

Similar results were also found with dissimilar welding of AA5083 to AA6082 by incorporation of TiC, CeMo and MWCNT nanoparticles forming equiaxed grains and concentric rich and poor regions in the WN. Moreover, the grain size was reduced by the TiC, CeMo and MWCNT by the pinning effect constricting the grain growth after the recrystallization [33,50]. However, the MWCNT nanoparticles in the joint had very fine harmonized grains in the WN and elongated grain size in the TMAZ region.

Studies have showed that welding parameters also enhance the grain and microstructure formation. The dissimilar joint had a grain size of 4 μm using TiC nanoparticles under high rotation speed with three passes along the same direction, where the grain size is smaller compared to the dissimilar Al joint reinforced with SiC nanoparticles [33,50]. This could be due to the welding parameters (i.e., high rotational speed, number of passes and direction change in the passes) as well as Ti particles for their higher atomic weight.

With the advantages of the high rotational speed of the tool reducing the grain size and improving the dispersion of nanoparticles, the high rotational speeds of tools also lead to deterioration of microstructures in AA6082 through high heat input. From the literature [81], it is shown that the β'' — Mg_5Si_6 precipitate in the AA6082 alloy has been strengthening and stable in a temperature below 200 $^\circ\text{C}$. However, with high rotational speed, the temperature reaches approximately 300 $^\circ\text{C}$, which tends to dissolve the β'' — Mg_5Si_6 precipitate and form the precipitate β' — $\text{Mg}_{1.7}\text{Si}$. In the stir zone of the dissimilar Al joints, the MgSi precipitate dissolved completely by the high heat; however, a small volume was found during the cooling time. With the small volume of MgSi in the stir zone, the mechanical properties were better compared to the AA6082 HAZ region. In the AA6082 HAZ region, the mechanical properties were drastically reduced. In addition to the Mg_5Si_6 and Mg_2Si intermetallic particles, other intermetallic particles such as Al, Mn and Mn_2Al_3 were also formed during the dissimilar Al welding, which did not have significant effect on the joint mechanical properties [50].

Thus, the grain size in the dissimilar Al joints was reduced by the incorporated nanoparticles through the pinning effect restricting the grain growth in the metal matrix. In addition, the improvised welding parameters such as high rotational speed of the tool, number and directional change in the passes enhance the grain growth reduction. However, these improvised welding parameters also led to dissolving of the strengthening intermetallic particles in AA6082 and precipitates along the grain boundaries.

3.3. Effect of Carbide Nanoparticles on Mechanical Properties

In AA5083 to AA6082 dissimilar joints without nanoparticle incorporation, the defect formation was reduced compared to the fusion welding process [76]. For the dissimilar joints of Al alloys through incorporating carbide nanoparticles, the grain size was further reduced in comparison to joints without reinforcement. According to the Hall–Petch relation, a decrease in grain size leads to an increase in the hardness property [23]. As the carbide (i.e., TiC and SiC) nanoparticles incorporated in the dissimilar Al joint had fine grain sizes compared to the joint without nanoparticles, the hardness was increased approximately 18% in the weld nugget. However, the hardness drastically reduced along the HAZ region of AA6082 [32,33]. This reduction was due to the dissolution of the β'' — Mg_5Si_6 precipitate and the increase in the hardness in the weld nugget was due to the formation of the new β' — $Mg_{1.7}Si$ precipitate [84]. In addition to the new precipitate formation improving the hardness, the reinforcing carbide nanoparticles also aided in improving hardness by their hard natures and pinning effect on the grain boundaries. The microhardness differences in the FSW dissimilar Al joints with addition of TiC and SiC nanoparticles are shown in Figure 17.

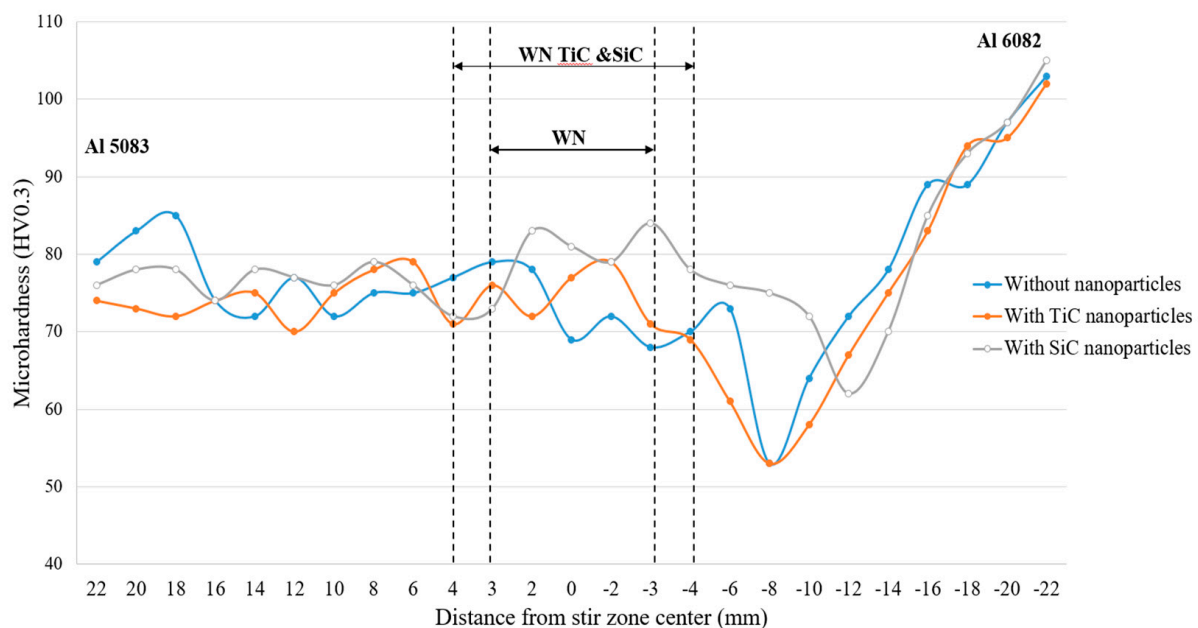


Figure 17. Microhardness distribution (2 mm under the surface) of the dissimilar Al joint reinforced with TiC nanoparticles, SiC nanoparticles and without nanoparticle addition.

From Figure 17, it can be seen that the joint reinforced with SiC nanoparticles has higher hardness in the weld nugget compared to the joints reinforced with TiC. Furthermore, the softening effect along the HAZ region in AA6082 is reduced compared to the joint reinforced with TiC nanoparticles. These variation in high hardness in WN could be due to the hard nature of SiC and the reduction in the softening effect on the AA6082 HAZ region could be due to the number of passes (i.e., two passes) causing low heat input in the joint.

Apart from the hardness, the ultimate tensile strength is another vital property for dissimilar joint integrity. Dissimilar Al joints without nanoparticle incorporation have average yield stresses and ultimate tensile strengths (UTSs) of approximately 140 and 193 MPa, respectively. Studies show that incorporating the TiC and SiC in FSW Al joints improved the tensile and yield strengths, which is shown in Table 4. This enhancement of the tensile strength was due to the SiC and TiC nanoparticle additions; however, the strengthening mechanism has to be researched. Moreover, the dissimilar Al joint with and without nanoparticles fractured at the HAZ region of AA6082, which could be due to the absences of nanoparticles and dissolution of strengthening precipitates [32,33,50]. In Table 4, it is shown that the SiC nanoparticles have a better effect on the tensile strength compared to TiC nanoparticles, which could be due to the SiC material having a higher yield and tensile strength. However, the FSW parameters also influence the tensile properties. For example, studies showed that the addition of TiC nanoparticles in dissimilar Al joints with changing directions in the passes reduced the ultimate tensile strength, which is lower than the joint without nanoparticle addition and thus leads to the fracture at the stir zone [33,50].

Table 4. Average tensile properties of joints without and with addition of TiC and with SiC nanoparticles.

Specimen	Young's Modulus (GPa)	Yield Stress (MPa)	UTS (MPa)	Elongation (%)
Without nanoparticles	65.5	140 ± 3	193 ± 3	3 ± 0.4
With SiC nanoparticles	78	138	217	5
With TiC nanoparticles	76.8	145 ± 2	199 ± 3	3.7 ± 0.3

In addition to the mechanical properties of the dissimilar Al joint, the corrosion resistance also plays a vital role in the joints, where these joints are used in shipbuilding and marine industries. The dissimilar Al joints are likely susceptible to localized corrosion, which could lead to pitting and intergranular corrosion. This occurs by dissolution of intermetallic particles along the grain boundaries in the joint [85]. I.A. Kartsonakis et al. [50] studied the influence of nanoparticle addition (i.e., TiC, MWCNT and CeMo) in the dissimilar Al joint, where the joints with TiC and MWCNT lead to pinholes and cavities on the surface when exposed to NaCl solution for 24 hr. However, the joint reinforced with CeMo nanoparticles acted as an inhibitor by dissolving as Ce and Mo ions, where the Ce formed as cerium hydroxide by the corrosive solution leading to a protective oxide film on the weld nugget.

This clearly shows that the dispersion of nanoparticles and the nature of nanoparticles with the aid of friction stir welding parameters such as number of passes and directional change improved the mechanical properties as well as corrosion resistance behavior. However, research is still needed for reducing the softening effect on AA6082 and further enhancement of the properties using other elements of nanoparticles.

4. Critical Analysis and Trends

Based on the review of available resources, the FSW welding parameters using nanoparticle reinforcement showed variations in joint formation in terms of rotation speed, traverse speed, number of passes and tool travel direction. Moreover, the type, size and amount of nanoparticles incorporated have a favorable effect on microstructural formation and joint properties.

Future perspectives have been progressing towards FSW reinforcement using nanoparticles, and only a limited resources are available.

- Even more research is required in FSW welding parameters, for correlating the type of nanoparticle reinforcement usage in the weld joint as well as base metal.
- As carbide and oxide nanoparticles possess high hardness properties, the selection of tool material is of paramount importance as it results in tool wear.

- Further research is needed on the reinforcement particles causing agglomeration in microstructural formation, which could be attained through FSW welding parameters (i.e., number of passes, high rotation and traverse speed).
- Studies are yet required on FSW of wide range of steel using nanoparticle reinforcement.

5. Discussion and Conclusions

Al alloys are attractive materials for various applications in shipbuilding, automobile and aerospace sectors, minimization of material weight and for joining complex structures with improved properties. Considering these industrial demands, the friction stir welding has been opted for rather than fusion welding processes due to the welding being conducted below melting temperature, reduction in defect formations as well as improved mechanical properties.

In 5x and 6x Al alloy series, AA5083 and AA6082 have been considered for use in various applications; however, friction stir welding of AA5083 and AA6082 still causes a reduction in joint strength. As studies showed that nanoparticle reinforcement in FSW improves properties, the carbide and oxide nanoparticles in similar and dissimilar welding of AA5083 and AA6082 showed improvements as well as the deterioration of joint property with the influence of welding parameters.

In the case of friction stir welding of AA5083:

- Homogeneous distribution of carbide nanoparticles (i.e., SiC and TiC) in joints requires slow traverse speed and high rotation speed; however, in the case of oxide nanoparticles (TiO₂), an increase in number of passes is required.
- The same intermetallic compounds were found in joints with and without nanoparticle reinforcement; however, the grain size was reduced compared to the joints without reinforcement particles.
- Hardness and ultimate tensile strengths have been improved compared to the joint without reinforcement; however, reductions in elongation and yield strengths have been noted. This could be due to the type of nanoparticle added.

For friction stir welding of AA6082:

- Carbide nanoparticles (i.e., SiC and TiC) had variations in friction stir welding parameters for uniform distribution, because of the physical properties of particles.
- Dilution of base metal intermetallic particles and new precipitation formation as well as same intermetallic particles were observed in joints with and without reinforcement. Amount of nanoparticle reinforcement has an influence on grain size formations.
- Improved mechanical properties of joints were achieved by increasing content of nanoparticle addition and the softening effect along the HAZ was reduced with nanoparticle reinforcement.

In dissimilar friction stir welding of AA5083 and AA6082:

- Rotational speed of the tool, number of passes and directional change greatly influenced dispersion of nanoparticles.
- Grain formation was equiaxed and the joint reinforced with TiC had small grain size compared to that with SiC. Dilution of strengthening precipitate occurred in AA6082.
- SiC nanoparticles improved joints' hardness, ultimate tensile strengths and elongation compared to joints with TiC and without reinforcement. Moreover, SiC reduced the softening effect on the HAZ region of AA6082. However, the joints with TiC had improved yield strengths.

A definitive reason for carbide nanoparticle reinforcement in similar and dissimilar AA5083 and AA6082 joints is the improved tensile properties by strengthening mechanisms; where the intermetallic compound formations are still not known. More research is required that investigates reductions in the softening effect on HAZ of AA6082, new intermetallic compound formations, subgrain formation mechanisms with nanoparticles and the factors influencing these formations as well as their effects on weld properties.

Author Contributions: C.V. wrote the entire manuscript, and corrected the manuscript following discussion with P.K. P.K. reviewed the draft for publication. All authors have read and agreed to the published version of the manuscript.

Funding: The research has been funded by University West, Sweden. Grant number 20200046. The project financier is Knowledge Foundation (KKS), Sweden.

Institutional Review Board Statement: Not applicable.

Informed Consent Statement: Not applicable.

Acknowledgments: The authors recognized the support by the Division of Welding Technology, Department of Engineering Science, The Production Technology Centre University West, SE-461 86 Trollhättan, Sweden.

Conflicts of Interest: The authors declare that there is no conflict of interest regarding publication of this paper.

Abbreviations

Al	Aluminum
Ce	Cerium
Cl	Chloride
Cr	Chromium
Cu	Copper
Fe	Iron
FSW	Friction Stir Welding
GMAW	Gas Metal Arc Welding
GTAW	Gas Tungsten Arc Welding
GPa	Giga Pascal
HAZ	Heat-Affected Zone
Mo	Molybdenum
Mg	Magnesium
MIG	Metal Inert Gas Welding
Mn	Manganese
MPa	Mega Pascal
MWCNT	Multiwall Carbon Nano Tube
Na	Sodium
RPM	Rotation per minute
SiC	Silicon Carbide
SZ	Stir Zone
TMAZ	Thermo-mechanically Affected Zone
TiC	Titanium Carbide
TIG	Tungsten Inert Gas Welding
TiO	Titanium Oxide
UTS	Ultimate Tensile Strength
WN	Weld nugget
Zn	Zinc
Zr	Zirconium

References

1. DuPont, J.N. Welding of Nickel-based alloys for energy applications. *Weld. J.* **2014**, *93*, 31–45.
2. Purslow, M.A. Reducing the ecological impact of arc welding: Practical strategies are offered for reducing energy consumption when using various arc welding processes. *Weld. J.* **2012**, *91*, 24–27.
3. Praveen, P.; Yarlagadda, P.K.D.V.; Kang, M.J. Advancements in pulse gas metal arc welding. *J. Mater. Process. Technol.* **2005**, *164–165*, 1113–1119. [[CrossRef](#)]
4. Soysal, T.; Kou, S. Effect of filler metals on solidification cracking susceptibility of Al alloys 2024 and 6061. *J. Mater. Process. Technol.* **2019**, *66*, 421–428. [[CrossRef](#)]
5. Lezzi, F.; Costa, L. The development of conventional welding processes in naval construction. *Weld. Int.* **2013**, *27*, 786–797. [[CrossRef](#)]

6. Liu, Z.; Ji, S.; Meng, X. Joining of magnesium and aluminum alloys via ultrasonic assisted friction stir welding at low temperature. *Int. J. Adv. Manuf. Technol.* **2018**, *97*, 4127–4136. [[CrossRef](#)]
7. Da Silva, C.L.M.; Scotti, A. The influence of double pulse on porosity formation in aluminum GMAW. *J. Mater. Process. Technol.* **2006**, *171*, 366–372. [[CrossRef](#)]
8. Jannet, S.; Mathews, K.; Raja, R. Comparative investigation of friction stir welding and fusion welding of 6061 T6-5083 O aluminum alloy based on mechanical properties and microstructure. *Bull. Pol. Acad. Sci. Tech. Sci.* **2014**, *62*, 791–795. [[CrossRef](#)]
9. Khaled, T. *An Outsider Looks at Friction Stir Welding*; Federal Aviation Administration: Washington, DC, USA, 2005; pp. 1–71. Available online: https://www.faa.gov/aircraft/air_cert/design_approvals/csta/publications/media/friction_stir_welding.pdf (accessed on 12 March 2019).
10. Mahoney, M.W.; Rhodes, C.G.; Flintoff, J.G.; Bingel, W.H.; Spurling, R.A. Properties of friction-stir-welded 7075 T651 aluminum. *Metall. Mater. Trans. A* **1998**, *29*, 1955–1964. [[CrossRef](#)]
11. Storjohann, D.; Barabash, O.M.; David, S.A.; Sklad, P.S.; Bloom, E.E.; Babu, S.S. Fusion and friction stir welding of aluminum-metal-matrix composites. *Metall. Mater. Trans. A* **2005**, *36*, 3237–3247. [[CrossRef](#)]
12. Mishra, R.S.; Mahoney, M.W.; Lienert, T.J.; Jata, K.V. Friction Stir Welding and Processing IV: Preface. In Proceedings of the TMS Annual Meet, Orlando, FL, USA, 25 February 2007.
13. Shi, L.; Wu, C.S.H.; Liu, J. The effect of the welding parameters and tool size on the thermal process and tool torque in reverse dual-rotation friction stir welding. *Int. J. Mach. Tools Manuf.* **2015**, *91*, 1–11. [[CrossRef](#)]
14. Miller, W.S.; Zhuang, L.; Bottema, J.; Wittebrood, A.J.; De Smet, P.; Haszler, A.; Vieregge, A. Recent development in aluminium alloys for the automotive industry. *Mater. Sci. Eng. A* **2000**, *280*, 37–49. [[CrossRef](#)]
15. Aluminium Alloys in the Automotive Industry: A Handy Guide. Available online: <https://aluminiuminsider.com/aluminium-alloys-automotive-industry-handly-guide/> (accessed on 4 May 2019).
16. Dursun, T.; Soutis, C. Recent developments in advanced aircraft aluminium alloys. *Mater. Des.* **2014**, *56*, 862–871. [[CrossRef](#)]
17. Aluminium in Shipbuilding. Available online: <http://www.aluminiumindustry.org/en/aluminium-shipbuilding.html> (accessed on 11 February 2009).
18. Mathers, G. *The Welding of Aluminium and Its Alloys*, 1st ed.; Woodhead Publishing: New York, NY, USA, 2002.
19. Tanaka, H.; Minoda, T. Mechanical properties of 7475 aluminum alloy sheets with fine subgrain structure by warm rolling. *Trans. Nonferrous Met. Soc. China* **2014**, *24*, 2187–2195. [[CrossRef](#)]
20. Calogero, V.; Costanza, G.; Missori, S.; Sili, A.; Tata, M.E. A Weldability Study of Al–Cu–Li 2198 Alloy. *Metallurgist* **2014**, *57*, 1134–1141. [[CrossRef](#)]
21. Koilraj, M.; Sundareswaran, V.; Vijayan, S.; Koteswara Rao, S.R. Friction stir welding of dissimilar aluminum alloys AA2219 to AA5083—Optimization of process parameters using Taguchi technique. *Mater. Des.* **2012**, *42*, 1–7. [[CrossRef](#)]
22. Dolatkah, A.; Golbabaee, P.; Besharati Givi, M.K.; Molaiekiya, F. Investigating effects of process parameters on microstructural and mechanical properties of Al5052/SiC metal matrix composite fabricated via friction stir processing. *Mater. Des.* **2012**, *37*, 458–464. [[CrossRef](#)]
23. Bahrami, M.; Dehghani, K.; Givi, M.K.B. A novel approach to develop aluminum matrix nano-composite employing friction stir welding technique. *Mater. Des.* **2014**, *53*, 217–225. [[CrossRef](#)]
24. Kianezhad, M.; Raouf, A.H. Effect of nano-Al₂O₃ particles and friction stir processing on 5083 TIG welding properties. *J. Mater. Process. Technol.* **2019**, *263*, 356–365. [[CrossRef](#)]
25. Kumar, N.; Yuan, W.; Mishra, R.S. Chapter 1—Introduction. In *Friction Stir Welding of Dissimilar Alloys and Materials*; Butterworth-Heinemann: Oxford, UK, 2015; pp. 1–13. [[CrossRef](#)]
26. Dimopoulos, A.; Vairis, A.; Vidakis, N.; Petousis, M. On the Friction Stir Welding of Al 7075 Thin Sheets. *Metals* **2021**, *11*, 57. [[CrossRef](#)]
27. Givi, M.K.B.; Asadi, P. *Advances in Friction-Stir Welding*; Woodhead Publishing: Cambridge, UK, 2014.
28. Heidarzadeh, A.; Khodaverdizadeh, H.; Mahmoudi, A.; Nazari, E. Tensile behavior of friction stir welded AA 6061-T4 aluminum alloy joints. *Mater. Eng.* **2012**, *37*, 166–173. [[CrossRef](#)]
29. Ceschini, L.; Boromei, I.; Minak, G.; Morri, A.; Tarterini, F. Effect of friction stir welding on microstructure, tensile and fatigue properties of the AA7005/10vol.%Al₂O₃p composite. *Compos. Sci. Technol.* **2007**, *67*, 605–615. [[CrossRef](#)]
30. Saeidi, M.; Barmouz, M.; Givi, M.K.B. Investigation on AA5083/AA7075+Al₂O₃ joint fabricated by friction stir welding: Characterizing microstructure, corrosion and toughness behavior. *Mater. Res.* **2015**, *18*, 1156–1162. [[CrossRef](#)]
31. Vimalraj, C.; Kah, P.; Mvola, B.; Martikainen, J. Effect of nanomaterial addition using gmaw and gtaw processes. *Rev. Adv. Mater. Sci.* **2016**, *44*, 370–382.
32. Pantelis, D.I.; Karakizis, P.N.; Daniolos, N.M.; Charitidis, C.A.; Koumoulos, E.P.; Dragatogiannis, D.A. Microstructural study and mechanical properties of dissimilar friction stir welded AA5083-H111 and AA6082-T6 reinforced with SiC nanoparticles. *Mater. Manuf. Process.* **2016**, *31*, 264–274. [[CrossRef](#)]
33. Dragatogiannis, D.A.; Koumoulos, E.P.; Kartsonakis, I.A.; Pantelis, D.I.; Karakizis, P.N.; Charitidis, C.A. Dissimilar Friction Stir Welding Between 5083 and 6082 Al Alloys Reinforced With TiC Nanoparticles. *Mater. Manuf. Process.* **2016**, *31*, 2101–2114. [[CrossRef](#)]

34. Scudino, S.; Liu, G.; Prashanth, K.G.; Bartusch, B.; Surreddi, K.B.; Murty, B.S.; Eckert, J. Mechanical properties of Al-based metal matrix composites reinforced with Zr-based glassy particles produced by powder metallurgy. *Acta Mater.* **2009**, *57*, 2029–2039. [[CrossRef](#)]
35. El Rayes, M.M.; Soliman, M.S.; Abbas, A.T.; Pimenov, D.Y.; Erdakov, I.N.; Abdel-mawla, M. Effect of Feed Rate in FSW on the Mechanical and Microstructural Properties of AA5754 Joints. *Adv. Mater. Sci. Eng.* **2019**, *2019*, 1–12. [[CrossRef](#)]
36. Bodaghi, M.; Dehghani, K. Friction stir welding of AA5052: The effects of SiC nano-particles addition. *Int. J. Adv. Manuf. Technol.* **2017**, *88*, 2651–2660. [[CrossRef](#)]
37. Tjong, S. Novel Nanoparticle-Reinforced Metal Matrix Composites with Enhanced Mechanical Properties. *Adv. Eng. Mater.* **2007**, *9*, 639–652. [[CrossRef](#)]
38. Paidar, M.; Asgari, A.; Ojo, O.O.; Saberi, A. Mechanical Properties and Wear Behavior of AA5182/WC Nanocomposite Fabricated by Friction Stir Welding at Different Tool Traverse Speeds. *J. Mater. Eng. Perform.* **2018**, *27*, 1714–1724. [[CrossRef](#)]
39. Ma, Z.Y.; Liu, B.L.; Xiao, W.G.; Wang, Z.Y. Tensile Strength and Electrical Conductivity of Carbon Nanotube Reinforced Aluminum Matrix Composites Fabricated by Powder Metallurgy Combined with Friction Stir Processing. *J. Mater. Sci. Technol.* **2014**, *30*, 649–655. [[CrossRef](#)]
40. Karakizis, P.N.; Pantelis, D.I.; Fourlaris, G.; Tsakiridis, P. Effect of SiC and TiC nanoparticle reinforcement on the microstructure, microhardness, and tensile performance of AA6082-T6 friction stir welds. *Int. J. Adv. Manuf. Technol.* **2018**, *95*, 3823–3837. [[CrossRef](#)]
41. Low, I.M. Nanoceramic Matrix Composites: Types, Processing, and Applications. In *Advances in Ceramic Matrix Composites, Australia*, 2nd ed.; Woodhead Publishing: Cambridge, UK, 2018.
42. Bahrami, M.; Nikoo, M.F.; Givi, M.K.B. Microstructural and mechanical behaviors of nano-SiC-reinforced AA7075-O FSW joints prepared through two passes. *Mater. Sci. Eng. A Struct. Mater. Prop. Microstruct. Process.* **2015**, *626*, 220–228. [[CrossRef](#)]
43. Hamdollahzadeh, A.; Bahrami, M.; Farahmand Nikoo, M.; Yusefi, A.; Besharati Givi, M.K.; Parvin, N. Microstructure evolutions and mechanical properties of nano-SiC-fortified AA7075 friction stir weldment: The role of second pass processing. *J. Manuf. Process.* **2015**, *20*, 367–373. [[CrossRef](#)]
44. Singh, T.; Tiwari, S.K.; Shukla, D.K. Mechanical and microstructural characterization of friction stir welded AA6061-T6 joints reinforced with nano-sized particles. *Mater. Charact.* **2020**, *159*, 110047. [[CrossRef](#)]
45. Sielski, R.A. Review of structural design of aluminum ships and craft. *Trans. Soc. Nav. Archit. Mar. Eng.* **2007**, *115*, 1–30.
46. Hakem, M.; Lebailli, S.; Miroud, J.; Bentaleb, A.; Toukali, S. Welding and characterization of 5083 aluminum alloy. In *METAL 2012—Conference Proceedings, 21st International Conference on Metallurgy and Materials*; Tanger Ltd.: Ostrava, Czech Republic, 2012.
47. Paik, J.K. Mechanical properties of friction stir welded aluminum alloys 5083 and 5383. *Int. J. Nav. Archit. Ocean Eng.* **2009**, *1*, 39–49. [[CrossRef](#)]
48. Klobcar, D.; Kosec, L.; Pietras, A.; Smolej, A. Friction-stir welding of aluminium alloy 5083. *Mater. Technol.* **2012**, *46*, 483–488.
49. Aval, H.J.; Loureiro, A. Effect of welding parameters on microstructure, mechanical properties and residual stress fields of friction stirwelds on AA5086. *Met. Mater.* **2016**, *53*, 51–58. [[CrossRef](#)]
50. Kartsonakis, I.A.; Dragatogiannis, D.A.; Koumoulos, E.P.; Karantonis, A.; Charitidis, C.A. Corrosion behaviour of dissimilar friction stir welded aluminium alloys reinforced with nanoadditives. *Mater. Des.* **2016**, *102*, 56–67. [[CrossRef](#)]
51. Jamalian, H.M.; Ramezani, H.; Ghobadi, H.; Ansari, M.; Yari, S.; Besharati Givi, M.K. Processing-structure-property correlation in nano-SiC-reinforced friction stir welded aluminum joints. *J. Manuf. Process.* **2016**, *21*, 180–189. [[CrossRef](#)]
52. Mirjavadi, S.S.; Alipour, M.; Emamian, S.; Kord, S.; Hamouda, A.M.S.; Koppad, P.G.; Keshavamurthy, R. Influence of TiO₂ nanoparticles incorporation to friction stir welded 5083 aluminum alloy on the microstructure, mechanical properties and wear resistance. *J. Alloys Compd.* **2017**, *712*, 795–803. [[CrossRef](#)]
53. Karakizis, P.N.; Pantelis, D.I.; Fourlaris, G.; Tsakiridis, P. The role of SiC and TiC nanoparticle reinforcement on AA5083-H111 friction stir welds studied by electron microscopy and mechanical testing. *Int. J. Adv. Manuf. Technol.* **2018**, *94*, 4159–4176. [[CrossRef](#)]
54. Mishra, R.S.; Ma, Z.Y. Friction stir welding and processing. *Mater. Sci. Eng. R Rep.* **2005**, *50*, 1–78. [[CrossRef](#)]
55. Palani, K.; Elanchezhian, C.; Saiprakash, K.H.V.; Sreekanth, K.; Dayanand, D.; Kumar, K.; Kumar, D. Effect of welding parameters on mechanical properties of dissimilar friction stir processed AA 8011 and AA 5083-H321 aluminium alloys. In *IOP Conference Series: Materials Science and Engineering*; IOP Publishing Ltd.: Tamilnadu, India, 2018. [[CrossRef](#)]
56. Elangovan, K.; Balasubramanian, V.; Valliappan, M. Effect of tool pin profile and tool rotational speed on mechanical properties of friction stir welded AA6061 aluminium alloy. *Mater. Manuf. Process.* **2008**, *23*, 251–260. [[CrossRef](#)]
57. Mirjavadi, S.S.; Alipour, M.; Hamouda, A.M.S.; Matin, A.; Kord, S.; Afshari, B.M.; Koppad, P.G. Effect of multi-pass friction stir processing on the microstructure, mechanical and wear properties of AA5083/ZrO₂ nanocomposites. *J. Alloys Compd.* **2017**, *726*, 1262–1273. [[CrossRef](#)]
58. Jata, K.V.; Sankaran, K.K.; Ruschau, J.J. Friction-stir welding effects on microstructure and fatigue of aluminum alloy 7050-T7451. *Metall. Mater. Trans. A Phys. Metall. Mater. Sci.* **2000**, *31*, 2181–2192. [[CrossRef](#)]
59. Shahraki, S.; Khorasani, S.; Abdi Behnagh, R.; Fotouhi, Y.; Bisadi, H. Producing of AA5083/ZrO₂ nanocomposite by friction stir processing (FSP). *Metall. Mater. Trans. B Process. Metall. Mater. Process. Sci.* **2013**, *44*, 1546–1553. [[CrossRef](#)]
60. Hoseinlghab, S.; Mirjavadi, S.S.; Sadeghian, N.; Jalili, I.; Azarbarmas, M.; Besharati Givi, M.K. Influences of welding parameters on the quality and creep properties of friction stir welded polyethylene plates. *Mater. Des.* **2015**, *67*, 369–378. [[CrossRef](#)]

61. Avettand-Fènoël, M.; Simar, A.; Shabadi, R.; Tailard, R.; De Meester, B. Characterization of oxide dispersion strengthened copper based materials developed by friction stir processing. *Mater. Des.* **2014**, *60*, 343–357. [[CrossRef](#)]
62. Scialpi, A.; De Filippis, L.A.C.; Cavaliere, P. Influence of shoulder geometry on microstructure and mechanical properties of friction stir welded 6082 aluminium alloy. *Mater. Des.* **2007**, *28*, 1124–1129. [[CrossRef](#)]
63. Hoyingchareon, K.; Muangjunburee, P. Welding repair of aluminium alloy 6082 T6 by TIG welding process. *Mater. Sci. Forum.* **2016**, *872*. [[CrossRef](#)]
64. Thimmaraju, P.; Arkanti, K.; Reddy, G.C.; Tilak, K.B.G. Comparison of microstructure and mechanical properties of friction stir welding of al 6082 aluminum alloy with different tool profiles. *Mater. Today Proc.* **2016**, *3*, 4173–4181. [[CrossRef](#)]
65. Muthukrishnan, M.; Marimuthu, M. Some studies on mechanical properties of friction stir butt welded al-6082-T6 plates. In Proceedings of the International Conference on Frontiers in Automobile and Mechanical Engineering (FAME), Material today, Chennai, India, 25–27 November 2010. [[CrossRef](#)]
66. Cavaliere, P.; Squillace, A.; Panella, F. Effect of welding parameters on mechanical and microstructural properties of AA6082 joints produced by friction stir welding. *J. Mater. Process. Technol.* **2008**, *200*, 364–372. [[CrossRef](#)]
67. El-Rayes, M.M.; El-Danaf, E.A. The influence of multi-pass friction stir processing on the microstructural and mechanical properties of Aluminum Alloy 6082. *J. Mater. Process. Technol.* **2012**, *212*, 1157–1168. [[CrossRef](#)]
68. Pantelis, D.I.; Karkizis, P.N.; Dragatogiannis, D.A.; Charitidis, C.A. Dissimilar Friction Stir Welding of Aluminum Alloys Reinforced with Carbon Nanotubes. In Nanomaterials in Joining. 2016. Available online: <https://www.scopus.com/inward/record.uri?eid=2-s2.0-84979178149&doi=10.1515%2f9783110339727-004&partnerID=40&md5=b1da077aafbc2afa4f2a4f5ff4016c5f> (accessed on 7 May 2019). [[CrossRef](#)]
69. Sing, S.K.; Rashid, M.; Kumar, D.; Kumar, S. Micro Structural and Mechanical Behaviours of Nano-TiC-Reinforced AA6082 FSW Joints. *Int. J. Trend Res. Dev. (IJTRD)* **2016**, *3*, 179–182.
70. Pityana, S. Microstructures of alloyed and dispersed hard particles in the aluminium surface. In Proceedings of the 4th Pacific International Conference on Applications of Lasers and Optics (PICALO), Wuhan, China, 23 March 2010.
71. Sun, Y.F.; Fujii, H. The effect of SiC particles on the microstructure and mechanical properties of friction stir welded pure copper joints. *Mater. Sci. Eng. A* **2011**, *528*, 5470–5475. [[CrossRef](#)]
72. Suresh, S.; Venkatesan, K.; Natarajan, E. Influence of SiC nanoparticle reinforcement on FSS welded 6061-T6 aluminum alloy. *J. Nanomater.* **2018**, *2018*. [[CrossRef](#)]
73. Tebyani, S.F.; Dehghani, K. Effects of SiC nanopowders on the mechanical properties and microstructure of interstitial free steel joined via friction stir spot welding. *Mater. Des.* **2016**, *90*, 660–668. [[CrossRef](#)]
74. Moradi, M.M.; Jamshidi Aval, H.; Jamaati, R.; Amirkhanlou, S.; Ji, S. Effect of SiC nanoparticles on the microstructure and texture of friction stir welded AA2024/AA6061. *Mater. Charact.* **2019**, *152*, 169–179. [[CrossRef](#)]
75. Luijendijk, T. Welding of dissimilar aluminium alloys. *J. Mater. Process. Technol.* **2000**, *103*, 29–35. [[CrossRef](#)]
76. Peel, M.J.; Steuwer, A.; Withers, P.J.; Dickerson, T.; Shi, Q.; Shercliff, H. Dissimilar friction stir welds in AA5083-AA6082. Part I: Process parameter effects on thermal history and weld properties. *Metall. Mater. Trans. A Phys. Metall. Mater. Sci.* **2006**, *37*, 2183–2193. [[CrossRef](#)]
77. Karlsson, L.; Larsson, H.; Bergqvist, E.L.; Stoltz, S. Friction stir welding of dissimilar al-alloys. In *Proceedings of the 2nd Friction Stir Welding Symposium*; TWI Ltd.: Cambridge, UK, 2000; pp. 281–290.
78. Reynolds, A.P.; Lockwood, W.D.; Seidel, T.U. Processing-property correlation in friction stir welds. *Mater. Sci. Forum.* **2000**, *331*, II. [[CrossRef](#)]
79. Jafari, H.; Mansouri, H.; Honarpisheh, M. Investigation of residual stress distribution of dissimilar Al-7075-T6 and Al-6061-T6 in the friction stir welding process strengthened with SiO₂ nanoparticles. *J. Manuf. Process.* **2019**, *43*, 145–153. [[CrossRef](#)]
80. Lee, S.; Shin, S.E.; Sun, Y.; Fujii, H.; Park, Y. Friction stir welding of multi-walled carbon nanotubes reinforced Al matrix composites. *Mater. Charact.* **2018**, *145*, 653–663. [[CrossRef](#)]
81. Peel, M.J.; Steuwer, A.; Withers, P.J. Dissimilar friction stir welds in AA5083-AA6082. Part II: Process parameter effects on microstructure. *Metall. Mater. Trans. A Phys. Metall. Mater. Sci.* **2006**, *37*, 2195–2206. [[CrossRef](#)]
82. Donatus, U.; Thompson, G.E.; Zhou, X.; Wang, J.; Cassell, A.; Beamish, K. Corrosion susceptibility of dissimilar friction stir welds of AA5083 and AA6082 alloys. *Mater. Charact.* **2015**, *107*, 85–97. [[CrossRef](#)]
83. Ji, S.D.; Shi, q.y.; Zhang, L.G.; Zou, A.L.; Gao, S.S.; Zan, L.V. Numerical simulation of material flow behavior of friction stir welding influenced by rotational tool geometry. *Comput. Mater. Sci.* **2012**, *63*, 218–226. [[CrossRef](#)]
84. Moreira, P.M.G.P.; Santos, T.; Tavares, S.M.O.; Richter-Trummer, V.; Vilaca, P.; De Castro, P.M.S.T. Mechanical and metallurgical characterization of friction stir welding joints of AA6061-T6 with AA6082-T6. *Mater. Des.* **2009**, *30*, 180–187. [[CrossRef](#)]
85. Montemor, M.F. Corrosion Issues in Joining Lightweight Materials: A Review of the Latest Achievements. In Nanomaterials in Joining. 2016. Available online: <https://www.scopus.com/inward/record.uri?eid=2-s2.0-84979176724&doi=10.1515%2f9783110339727-005&partnerID=40&md5=4f572286bbfa2e77eb7e76998f241c8f> (accessed on 4 May 2019). [[CrossRef](#)]